THE PHOTOCHEMISTRY OF SOME QUADRATE Cr(III) COMPLEXES

by

JOHN GWYNFRYN VALENTIN

B.Sc., University of British Columbia, 1964

A THESIS SUBMITTED IN PARTIAL FULFILLMENT

OF THE REQUIREMENTS FOR THE DEGREE OF

MASTER OF SCIENCE

in the Department

of

Chemistry

Accepted 8 September 1970

[redacted]

Dean, Faculty of Graduate Studies

We accept this thesis as conforming

to the required standard

[redacted]

UNIVERSITY OF VICTORIA

August 1970

ERRATA

1. p. ii - line 4 - "spacial" should read "spatial".
2. p. 11 - line 11 - "first four Russell-Saunders states" should read "first three Russell-Saunders states".
3. p. 22 - line 8 - "two empirical rules" should read "a number of empirical rules".
4. p. 32 - line 4 - "Quartz lense" should read "Quartz lens".
5. p. 43 - line 17 - "additonal" should read "additional".
6. p. 45 - line 18 - "kown" should read "known".
7. p. 51 - line 11 - "Schläfer et al found" should read "Schläfer et al (17) found".

   line 17 - "cis-$[Cr(enH)(H_2O)(ox)_2]^-$" should read "cis-$[Cr(enH)(H_2O)(ox)_2]^o$".
8. p. 65 - line 21 - "series of complex" should read "series of complexes".
9. p. 71 - line 18 - "firt 8%" should read "first 8%".
10. p. 78 - line 9 - "increasing ΔE" should read "increasing Δ".
11. p. 83 - line 12 - "de-excitation process" should read "de-excitation processes".

Supervisor: Professor A.D. Kirk

ABSTRACT

The aquation quantum yields of $[Cr(en)_2ox]^+$, $[Cr\ en(ox)_2]^-$, cis-$[Cr(en)_2Cl_2]^+$ and trans-$[Cr(en)_2Cl_2]^+$ were measured in the visible region at pH 3.0 and at various wavelengths and temperatures. The results are interpreted in terms of empirical rules proposed by earlier workers.

Both $[Cr(en)_2ox]^+$ and $[Cr\ en(ox)_2]^-$ were found to give protonated monodentate ethylenediamine complexes as primary photolysis products. The $\phi_a(en)$ were found to be $(1.6 \pm .2) \times 10^{-1}$ and $(2.0 \pm .9) \times 10^{-2}$ respectively. No oxalate photoaquation was observed for either complex.

Cis-$[Cr(en)_2Cl_2]^+$ was found to undergo both ethylenediamine and Cl^- photoaquation with $\phi_a(en) = (1.3 \pm .2) \times 10^{-1}$ and $\phi_a(Cl^-) = (1.5 \pm 1.0) \times 10^{-2}$. Trans-$[Cr(en)_2Cl_2]^+$ showed only Cl^- aquation with $\phi_a(Cl^-) = (3.2 \pm .2) \times 10^{-1}$.

It was found that photoaquation of $[Cr\ en(ox)_2]^-$ and trans-$[Cr(en)_2Cl_2]^+$ was accompanied by stereochemical changes, requiring water attack trans to the leaving group.

PREFACE

Photochemical reactions of a molecule or ion are those reactions induced by the absorption of a quantum of light. In some cases the absorbed quantum of light supplies the energy to directly induce the reactions by rupturing bonds and in others it changes the spacial or electronic configuration of the molecule or ion making it more susceptible to attack by surrounding molecules or ions.

Understanding the mechanisms of photochemical reactions requires knowledge of the structure of the reactant, some information about its thermal reactions and perhaps most important an understanding of its spectroscopy or, what happens to the molecule or ion in the short time between absorption of light and photochemical reaction. Of course, it should be understood that absorption of light does not necessarily produce a photochemical reaction as other processes can occur (phosphorescence, fluorescence, radiationless transitions, etc.).

This work is concerned with the photochemical reactions of Cr(III) coordination complexes. With the above in mind it has been chosen to introduce the topic by presenting brief discussions about first, the structure and thermal reactions of transition metal coordination complexes, then a general introduction to photochemistry, followed by a brief discussion of ligand field theory as applied to Cr(III). With the foregoing as background the photochemistry of Cr(III) complexes is introduced.

TABLE OF CONTENTS

LIST OF TABLES

LIST OF FIGURES

ABBREVIATIONS AND SYMBOLS

en - ethylenediamine

(A-A) - bidentate ligand - a ligand with two sites that can coordinate to the central atom simultaneously.

ϕ_a - photochemical quantum yield for aquation.

ϕ_i - photochemical quantum yield for isomerization.

ϕ_r - photochemical quantum yield for racemization.

ϕ_t - total photochemical quantum yield

$$\phi_t = \phi_a + \phi_i + \phi_r$$

$h\nu$ - represents one quantum of light

$^4T_{2g} \dashrightarrow {}^4A_{2g}$ - straight arrow between two spectroscopic states indicates a radiative transition.

$^4T_{2g} \rightsquigarrow {}^4A_{2g}$ - crooked arrow indicates a non-radiative transition.

ox - oxalate anion

ACKNOWLEDGEMENTS

The author wishes to express his thanks to Drs. A. D. Kirk and K. C. Moss for their patient guidance during the course of this work, and to the National Research Council for grants making the work possible.

Special thanks to Elke for meticulously typing this thesis.

I. INTRODUCTION TO COORDINATION CHEMISTRY

A. Definition of Coordination Complexes

Transition metal coordination complexes can loosely be defined as compounds consisting of a central transition metal atom or ion with a cluster of surrounding molecules or ions. The coordinated groups surrounding the metal can be anionic, neutral or cationic. Examples of transition metal complexes include $[Pt(NH_3)_2(Cl)_2]$, $[Cr(CN)_6]Cl_3$ and $[Co(NH_3)_5Cl]Cl$.

During the latter part of the 19th century a number of various attempts were made to systematize the observed reactions and propose structures for what was at that time a new class of compounds. At the turn of the century Alfred Werner, working with the complexes of Co, Pt, and Cr, conceived the idea that the central atom has two types of valency - "primary" and "secondary". In today's terminology Werner's secondary valence is equivalent to the coordination number of the central atom or the number of ligands accommodated in the coordination sphere (usually four or six). The primary valence is the normal ionic charge associated with the central metal ion and can be satisfied only by negative ions.

Thus the structure of $Co(NH_3)_5Cl_3$ that had been postulated by S. M. Jorgensen to be

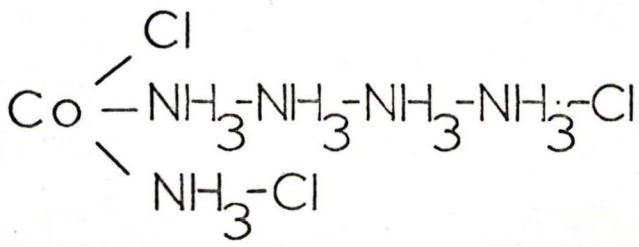

was correctly interpreted by Werner to be

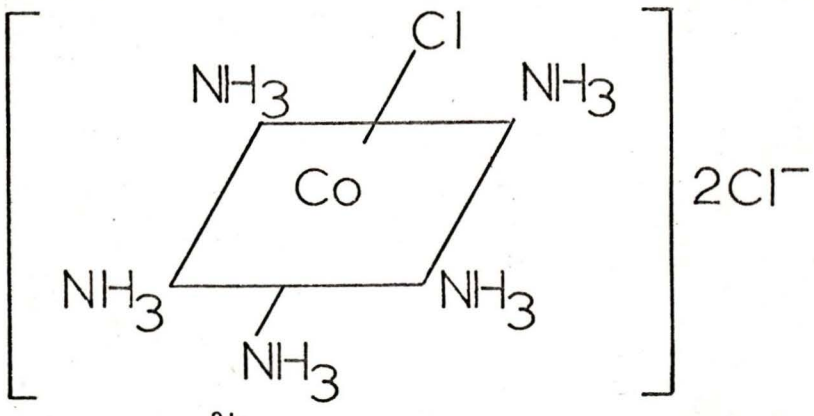

- a Co^{3+} metal ion surrounded by an octahedral array of five NH_3 molecules and one Cl^- ion. The dipositive charge of the complex ion is neutralized by two Cl^- ions outside the coordination sphere (1). To emphasize this structure we now write the formula $[Co(NH_3)_5Cl]Cl_2$ where the coordination sphere is indicated by [ ].

Werner also postulated that the secondary valence bonds were directed in space and thus allowed for the possibility of geometrical isomers. The existence of such isomers was later established by Werner by his preparation of cis and trans-$[Co(NH_3)_4Cl_2]Cl$. In 1913 Werner was awarded the Nobel Prize for his work in coordination chemistry.

B. Symmetry of Coordination Complexes

Although transition metal complexes with coordination numbers of two, three, five, seven, eight and higher are known to exist, by far the largest number, especially in the first transition series, have coordination numbers of four and six. Coordination number four

gives rise to either square planar or tetrahedral configurations, while coordination number six gives rise to octahedral configurations which are sometimes modified by tetragonal or trigonal distortions.

Since the bulk of the ensuing discussion concerns octahedral complexes some mention of the symmetry designations is necessary. An octahedral complex having six equivalent ligands belongs to the symmetry class O_h. In this work complexes with six ligands all of which are not equivalent will be designated as non-O_h. Although they have the overall symmetry of an O_h complex and, to a first approximation, can be treated theoretically as belonging to the O_h symmetry class, in some cases their spectral properties are different from those of O_h complexes and the distinction must be made.

C. Reactions of Octahedral Coordination Complexes

Apart from oxidation-reduction reactions, which will not be considered, the reactions of octahedral coordination compounds can roughly be divided into the following classes:

1. Substitution Reactions

$$[ML_6]^{n+} + H_2O \longrightarrow [ML_5(H_2O)]^{n+} + L \text{ (solvolysis)} \qquad (1)$$

$$[ML_6]^{n+} + X^- \longrightarrow [ML_5X]^{(n-1)+} + L \text{ (anation)} \qquad (2)$$

where M = metal atom or ion

L = ligand

X^- = anionic ligand

The rates of the substitution reactions can vary greatly depending on the central metal ion and the type of ligand surrounding it. The terms lability and inertness for a complex ion describe the rate at which it undergoes substitution reactions. Generally complexes that undergo substitutions with half-lives of about a minute or less are termed labile and all others are termed inert. Of the ions in the first transition metal series only Cr(III) and Co(III) form a large number of inert octahedral complexes. Cr(III) and Co(III) complexes undergo substitution reactions with half-lives in the order of a few hours to a few days at 25°C. This factor along with others makes the octahedral complexes of these ions very convenient for kinetic study.

Substitution reactions of octahedral complexes can go by S_N1 (five coordinate intermediate) or S_N2 (seven coordinate intermediate) mechanisms, but the assignment of a particular mechanism to a reaction is sometimes very difficult. Both mechanisms can lead to products with stereochemistries different from that of the reactant (2).

2. Isomerization Reactions

$$\text{cis-}[ML_4X_2]^{n+} \longrightarrow \text{trans-}[ML_4X_2]^{n+} \qquad (3)$$

3. Racemization Reactions

$$\text{dextro-}[M(A\text{-}A)_2L_2]^{n+} \longrightarrow \text{levo-}[M(A\text{-}A)_2L_2]^{n+} \qquad (4)$$

where A-A is a bidentate ligand

Racemization reactions can occur by two different mechanisms,

one involving bond breaking followed by reforming of the bond and the other involving a twist mechanism where no bond breaking is involved (3).

4. Reactions of the Coordinated ligands that do not involve the metal ligand bond

$$[Cr(en)_2(H_2O)_2]^{3+} \rightleftharpoons [Cr(en)_2(H_2O)OH]^{2+} + H^+ \quad (5)$$

Except for the acid base equilibria, which do not occur photochemically, all of the above types of reactions can be induced in at least some octahedral Cr(III) complexes both thermally and photochemically.

II. INTRODUCTION TO PHOTOCHEMISTRY

Photochemical investigations date back more than a century to Grotthus and Draper who formulated the first law of photochemistry - "Only light which is absorbed by a molecule can be effective in producing a photochemical change in the molecule." The second law of photochemistry was deduced by Stark (1908-12) and Einstein (1912-13) - "The absorption of light by a molecule is a one-quantum process so that the sum of the primary process quantum yields must be unity." This is known as the Einstein Law of Photochemical Equivalence. The primary processes may include dissociation, isomerization, fluorescence, phosphorescence, radiationless transitions and all other reaction paths that lead to the deactivation of the excited molecule.

The quantum yield (ϕ) for the reaction

$$[A] + h\nu \longrightarrow [B] \qquad (6)$$

is defined as

$$\phi = \frac{\text{molecules of B formed per unit volume per unit time}}{\text{quanta of light absorbed by A per unit volume per unit time}}$$

Photochemical reactions or processes are of importance in a variety of situations; photosynthesis, photography, fading or bleaching of dyes and other substances by sunlight and suntanning are all processes involving photochemistry.

Most of the investigations into photochemical reactions have been

concerned with organic systems. The known number and type of such reactions is very large and growing continuously. A great deal of work has also been done on the photochemistry of inorganic gases such as ozone, HCl, and the oxides of nitrogen, as well as in the area of photography where the photochemistry of ionic silver salts is very important.

Until the last decade very little serious study of transition metal complexes had been undertaken although the photosensitivity of a number of these complexes had been observed for many years. The main concern of early workers was that the photochemical reactions interfered with their attempts to study thermal kinetics and they found it necessary to do much of their work in the dark (similar to conditions under which much of this work was done).

However, the development of ligand field theory has now led to a fuller understanding of the excited states and excited state processes of transition metal complexes, and this has in turn led to the recent increase in interest in transition metal photochemistry.

A substantial number of transition metals form complexes that have now been shown to undergo photochemical reactions. Adamson et al (4) published a review in 1968 covering most of the known transition metal photochemistry of the first, second and third row transition metals and several of the lanthanides and actinides. The main photochemical processes involve oxidation or reduction of the metal centre or substitution of one of the ligands.

III. THEORY

A. Transition Metals and the Ligand Field Theory

1. Atomic Orbitals

In what follows it is assumed that the reader is familiar with the quantum mechanics of atomic systems at the level of works such as ref. 16. As is well known, the approximate order of filling of the atomic orbitals for the elements up to the end of the first row transition metals is 1s, 2s, 2p, 3s, 3p, 4s, 3d. The order of the 4s and 3d levels is dependent on the particular element and its oxidation state. Transition metals are those elements with partially filled d-orbitals in any of their oxidation states.

2. One Electron in the d Levels

The following discussion assumes one electron in the 3d level of a transition metal ion in the gas phase and in the absence of any external perturbations. An electron in the 3d level can exist in five different states (orbitals) of equal energy (degenerate) designated $d_{x^2-y^2}$, d_{z^2}, d_{xy}, d_{xz}, d_{yz}.

When the metal ion is surrounded by an octahedral array of six ligands the d orbitals are all raised in energy and are split by the electronic interaction between the ligands and the d-orbitals. The $d_{x^2-y^2}$ and d_{z^2} orbitals are thought of as pointing toward the ligands and are higher in energy relative to the d_{xy}, d_{xz}, d_{yz} orbitals which are thought of as pointing between the ligands. Fig. 1 illustrates

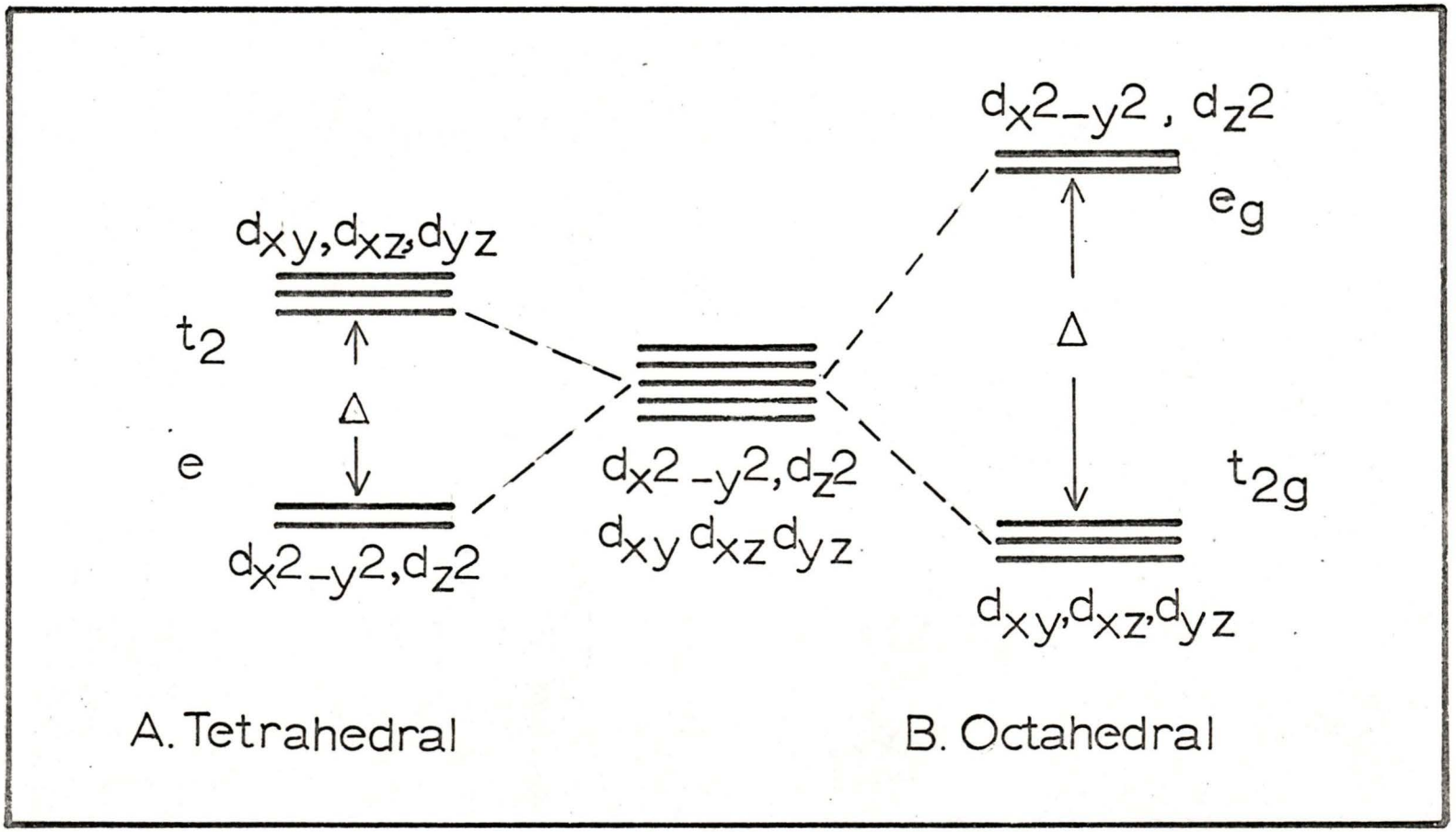

FIGURE 1. Splitting of d-orbitals by Tetrahedral and Octahedral Arrays of Ligands

the splitting due to the octahedral ligand field. Similar splittings are observed for other arrangements of various numbers of ligands and the splitting due to tetrahedral fields is also displayed in Fig. 1.

For the octahedral case symmetry considerations have led to the designation of the higher energy level as the e_g (doubly degenerate) level and the lower level as the t_{2g} (triply degenerate) level. The two levels are separated by an energy difference Δ. The magnitude of Δ is dependent on the type of ligand and the metal ion and on basis of theory can be obtained from the visible absorption spectrum of the complex. Ligands that produce a strong electronic interaction with the d orbitals of the central metal ion, give large values of Δ and those with weak interactions give small values of Δ. The common ligands have been arranged in a series according to their ability to split the d levels. Ligands that lie high on this spectrochemical series are termed strong field ligands and those that lie low on the series are weak field ligands. The ligands discussed in this work lie in the following order with respect to their ligand field strength (6).

$$en > NH_3 > H_2O \simeq ox > urea > Cl^-$$

3. More than One Electron in the d Level

When more than one electron is in the d level interelectronic repulsions must be considered. Two independent procedures for calculating the ligand field splittings can be used. Both lead to the same result. In the following the free Cr(III) atom is first considered and then the effects of a "weak" ligand field and a "strong" ligand field on the energy states of the free atom. The d^3 configuration

is used as an example since this applies directly to Cr(III). Fig. 2 shows the correlation between the weak field and strong field approximations.

a. Free Cr(III) Atom

In the absence of any external perturbations the three electrons of the d^3 configuration interact by interelectronic repulsion and the degeneracy of the d level is removed. The energy states (terms) available to the electron are found by considerations of the coupling between the total spin angular momentum and the total orbital angular momentum of the electrons (Russell-Saunders coupling). In the d^3 case the first four Russell-Saunders states are, in order of increasing energy, ^4F, ^4P and ^2G (Fig. 2). The energy spacings between the terms can be calculated in terms of the interelectronic repulsion parameters B and C (Racah parameters). Thus Ballhausen (15) expresses the energy difference between ^4F and ^2G for example as:

$$E(^4F\text{-}^2G) = 4B + 3C$$

b. Weak Field Approximation

Just as the d orbitals are split by interactions with the ligand field in the one electron case, so are the Russell-Saunders states of the d^3 configuration. In the weak field approximation the ligand field splitting of the Russell-Saunders states is thought of as being small compared to the energy differences between the states. Thus in the weak field approximation the Russell-Saunders states are first calculated and then the ligand field splitting applied. Calculation shows for example that the ^4F state gives rise to $^4A_{2g}$, $^4T_{1g}$ and $^4T_{2g}$ states in the presence of a ligand field (Fig. 2).

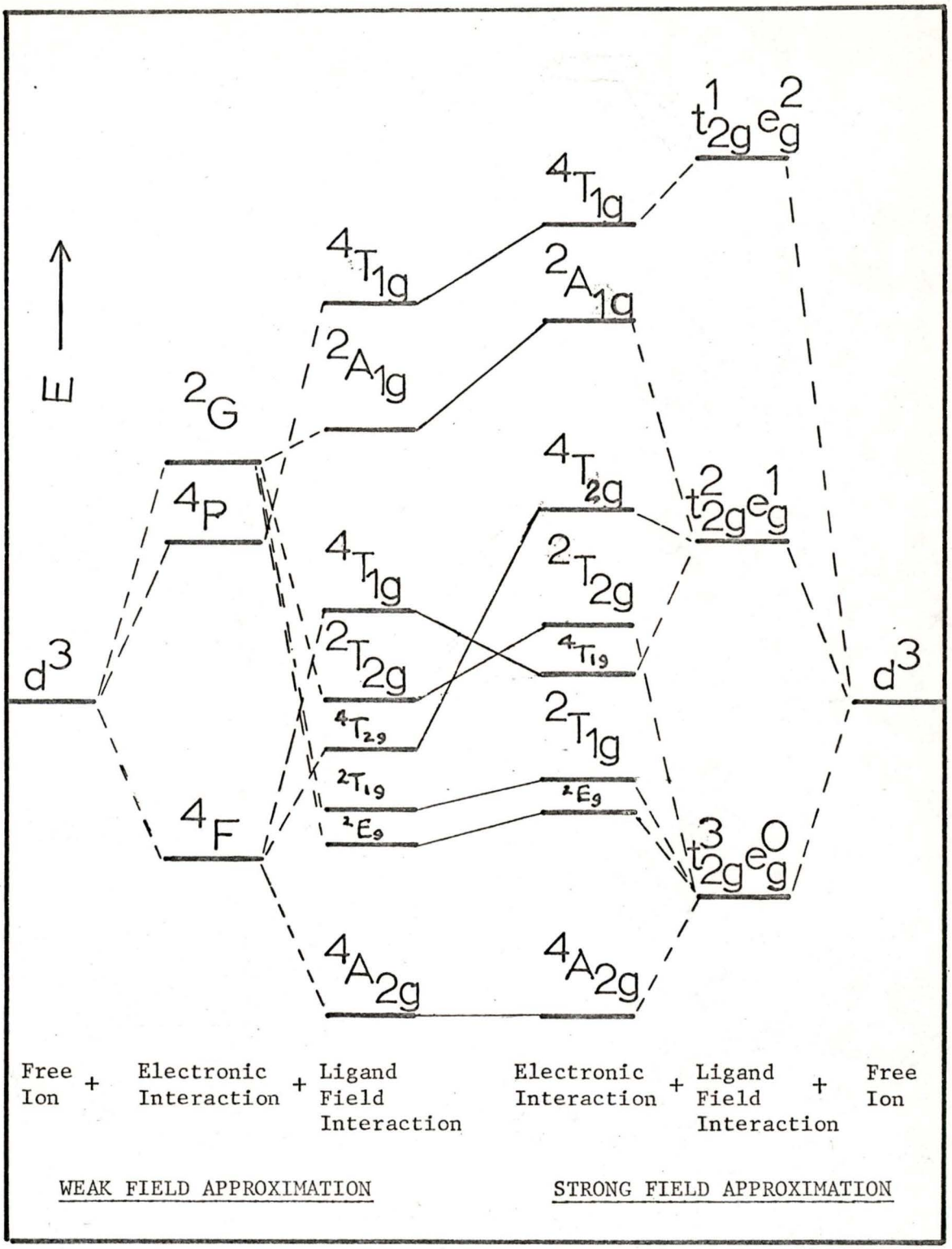

FIGURE 2. Weak Field and Strong Field Approximations to d-Level Splitting of a Cr(III) Ion in an O_h Ligand Field. (Not to Scale.)

c. Strong Field Approximation

In the strong field approximation the splitting due to the ligand field is thought of as being larger than the splitting due to inter-electronic repulsions. In this approximation the energy levels of the various electronic configurations [for example (t_{2g}^3, e_g^0), (t_{2g}^2, e_g^1), (t_{2g}^1, e_g^2)] are calculated and then these are considered to be split by the interelectronic repulsions.

It turns out that the same set of energy levels is derived using either the weak field approximation or the strong field approximation if the calculations are taken to completion.

d. The Tanabe-Sugano Diagram (Fig. 3)

The Tanabe-Sugano diagram allows interpretation of the energy levels obtained in the real cases of intermediate fields. On the extreme left hand side of the Tanabe-Sugano diagram are the Russell-Saunders terms for the free ion. Δ, the ligand field strength, increases to the right of the diagram and as Δ increases it can be seen that the Russell-Saunders states are split into new states, the symbols for which arise from symmetry theory. The superscripts on the term symbols define the spin multiplicity of the state.

E/B is plotted against Δ/B on these diagrams so that they can be used for any complex ion of d^3 configuration regardless of the value of B for that ion. The position of the terms on the diagram is dependent on the two variables Δ and B so that to plot both of these against E would require a three dimensional diagram.

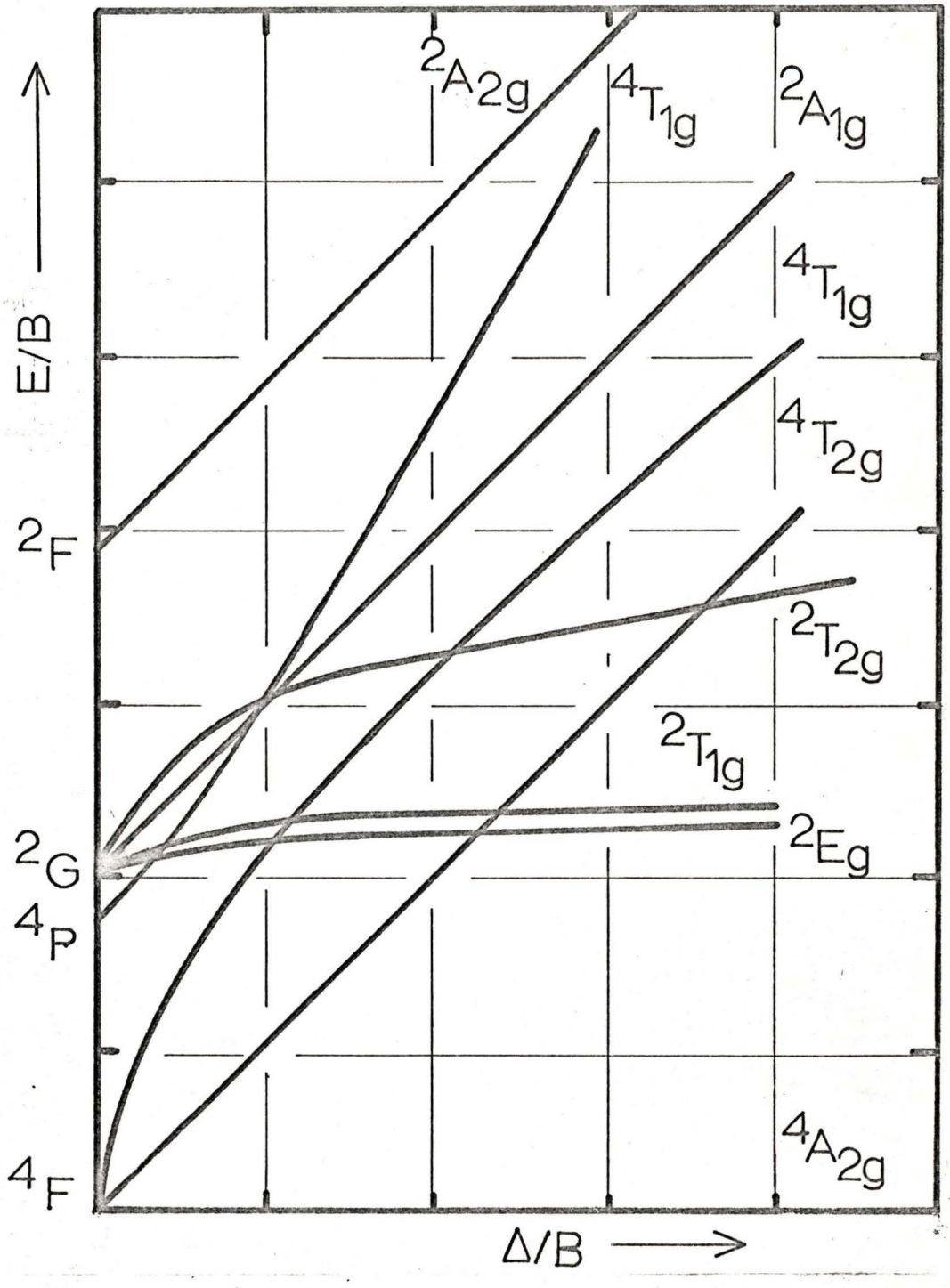

FIGURE 3. Tanabe-Sugano Diagram of d^3 System

The Tanabe-Sugano diagrams are mainly used in the assignment of absorption bands of coordination complexes.

B. The Absorption Spectra of Cr(III) Complexes

Knowledge of the absorption spectra of the complexes is necessary so that suitable wavelengths can be used for photolysis experiments.

Referring to Fig. 3, $^4A_{2g}$ is seen to be the ground state of the d^3 configuration. The ^2E_g, $^2T_{1g}$ and $^2T_{2g}$ states arise from spin pairing in the (t_{2g}^3, e_g^0) strong field configuration and the $^4T_{2g}$ and $^4T_{1g}$ states arise from the (t_{2g}^2, e_g^1) strong field configuration. There are higher states as Fig. 3 shows but they need not be considered for the ensuing discussion.

The lowest energy transitions in the complex correspond to absorption of visible light causing the excitation of an electron from the t_{2g} to the e_g level. This is the source of the characteristic absorptions ($^4T_{1g} \leftarrow {}^4A_{2g}$, $^4T_{2g} \leftarrow {}^4A_{2g}$) of Cr(III) complexes in the visible region (Fig. 4). Both these transitions are parity forbidden and thus exhibit low intensity ($\varepsilon_{max}<100$). The absorption bands are broad with no vibrational structure. In addition to these there are the observed spin pairing transitions between the ^2E_g, $^2T_{1g}$ and $^4A_{2g}$ states. Most commonly seen is the transition $^2E_g \leftarrow {}^4A_{2g}$ which is both Laporte forbidden and spin forbidden and thus exhibits a very low intensity absorption band ($\varepsilon_{max}<0.1$). These bands are quite narrow

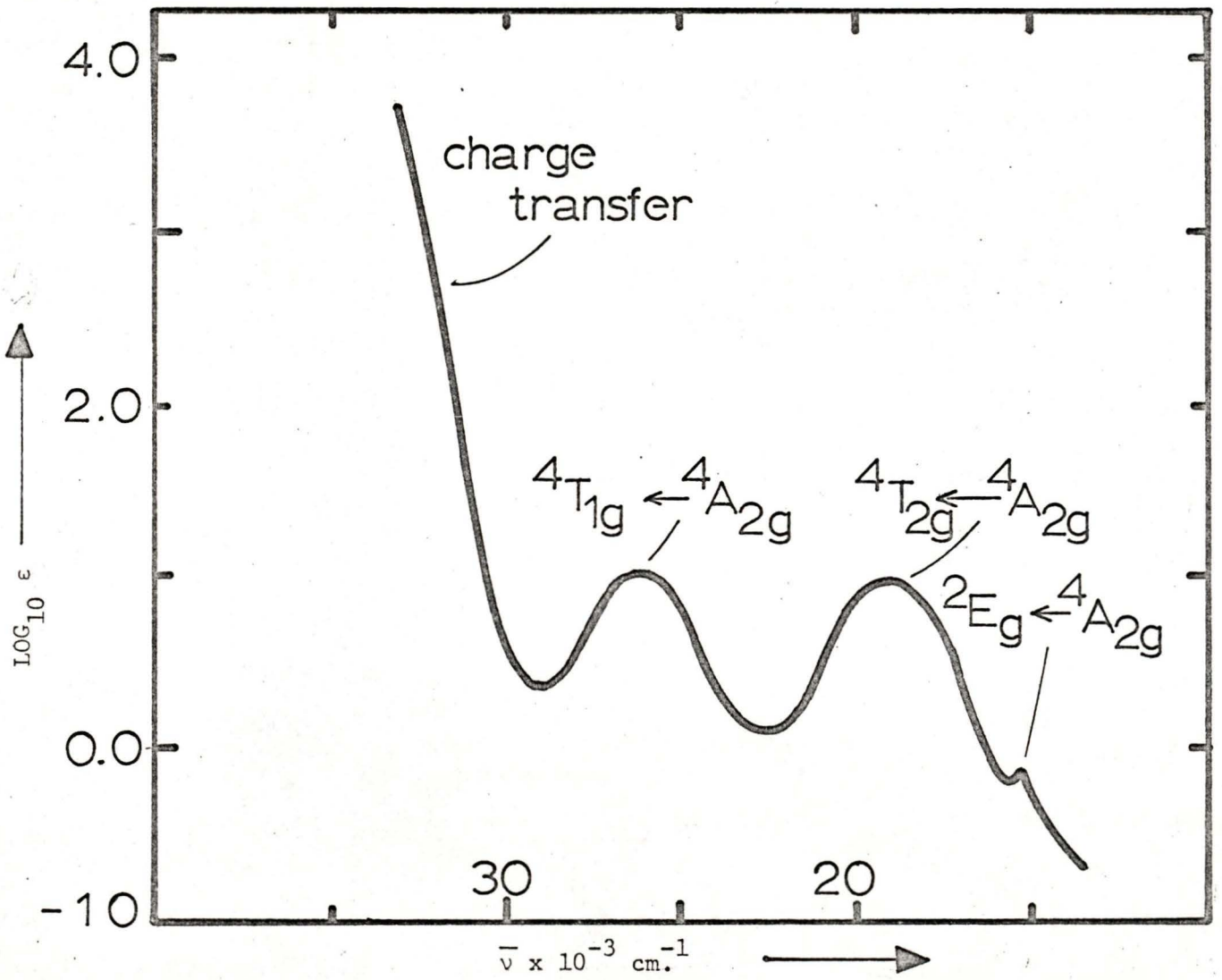

FIGURE 4. Typical Visible and Near U.V. Absorption Spectrum of a Cr(III) Complex

and show some vibrational structure. Finally a very high intensity charge transfer band extends well into the ultra-violet region. This corresponds to the transition of an electron from a ligand to the metal ion.

C. Excited State Processes of Cr(III) Complex Ions

Fig. 5 shows an idealized potential energy level diagram for the firsttwo excited states of a d^3 system, and also the definition of Δ, ΔE and ΔE_o. Because of the Franck-Condon principle (appendix 1) absorption of visible light in one of the quartet bands results in excitation to a high vibrational level of an electronically excited state. Excitation to the $^4T_{2g}$ state is followed by rapid thermal equilibration to the lowest vibrational level. Population of ^2E_g can occur by intersystem crossing from $^4T_{2g}$ to ^2E_g and the reverse ($^4T_{2g} \leftsquigarrow {}^2E_g$) can also occur. Phosphorescence ($^2E_g \rightarrow {}^4A_{2g}$) is observed at low temperatures for most Cr(III) complexes, but fluorescence ($^4T_{2g} \rightarrow {}^4A_{2g}$) only in the few cases where the zeroth vibrational level of $^4T_{2g}$ lies very near or below ^2E_g.

The lifetime of the excited states and some insight into their configuration can be determined from close examination of the luminescence properties. Information of this type is important in the identification of which of $^4T_{2g}$ or ^2E_g is the state from which photochemical reactions occur.

More detailed accounts of Cr(III) excited state processes are given in the reviews by Adamson (4), Valentine (5) and Forster (7).

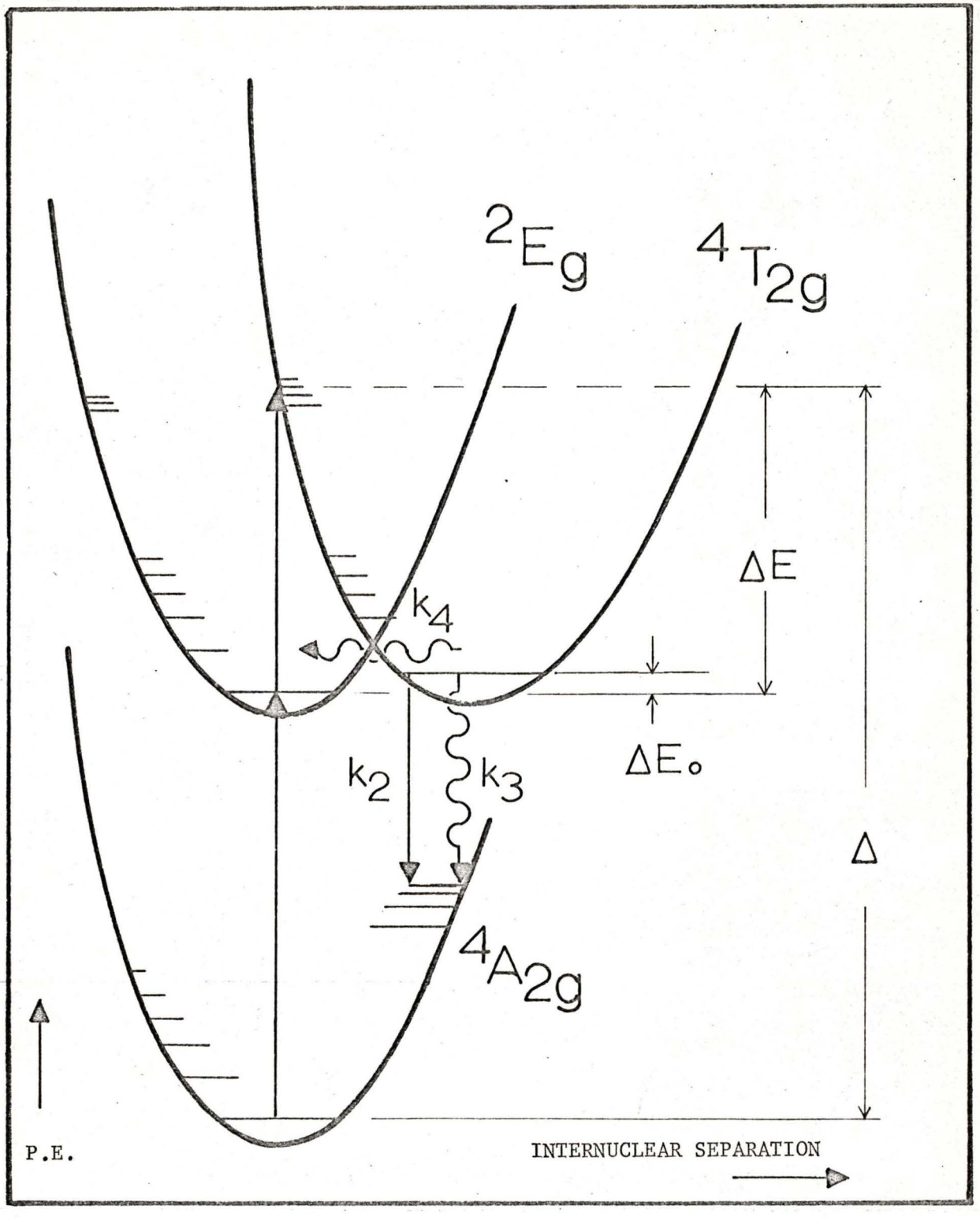

FIGURE 5. Potential Energy Diagram of First Two Excited States of Cr(III) ion in O_h Ligand Field.

IV. INTRODUCTION TO Cr(III) PHOTOCHEMISTRY

A. Advantages of Cr(III) Complexes for Photochemical Studies

Cr(III) complexes lend themselves ideally to a study of photochemical substitution reactions. Besides being kinetically inert, Cr(III) complexes, unlike those of Co(III), do not undergo complicated redox reactions in aqueous solution. A great deal of work has been carried out on the luminescence properties of Cr(III) and as a result the excited states and excited state processes are fairly well understood. Well resolved d-d absorption bands allow excitation to known electronic states if monochromatic light is used. Finally, the availability of a large variety of complexes from literature sources allows the testing of proposed photochemical relationships between different compounds.

B. Photochemical Reactions of Cr(III) Complexes

Consider the following example of photochemical reactions assuming a cis-dextrorotatory isomer of a non-O_h Cr(III) complex. Since this work is mainly concerned with compounds containing bidentate ligands, bidentate ligands are used in the example.

Absorption of visible light produces an electronically excited ion that has a measurable lifetime and can exist in either the ^2E_g or $^4T_{2g}$ state.

$$\text{cis-d-}[Cr(A\text{-}A)_2X_2]^{n+} \rightarrow \text{cis-d-}[Cr(A\text{-}A)_2X_2]^{n+\,*} \qquad (7)$$

One of the ligands in the excited ion may be labilized. The excited ion can react by:

$$\text{cis-d-}[Cr(A\text{-}A)_2X_2]^{n+*}$$

$$\rightarrow \text{cis-l-}[Cr(A\text{-}A)_2X_2]^{n+} \text{ (racemization)} \quad (8)$$

$$\rightarrow \text{trans-}[Cr(A\text{-}A)_2X_2]^{n+} \text{ (isomerization)} \quad (9)$$

$$\rightarrow [Cr(A\text{-}A)_2(H_2O)X]^{(n+1)+} + X^- \text{ (aquation)} \quad (10)$$

$$\rightarrow [Cr(A\text{-}A)(H_2O)_2X_2]^{n+} + (A\text{-}A) \text{ (aquation)} \quad (11)$$

The total quantum yield is given by:

$$\phi_{total} = \phi_a + \phi_i + \phi_r$$

where ϕ_a = aquation quantum yield

ϕ_i = isomerization quantum yield

ϕ_r = racemization quantum yield

In the cases where more than one reaction occurs there is no reason to assume that each reaction goes by the same mechanism, or from the same excited state.

C. ^2E_g or $^4T_{2g}$ as the Precursor in Cr(III) Photochemistry

Central to the investigation of Cr(III) photochemistry is the identification of the excited state or states responsible for the photochemical reactions. There are conflicting points of view, one side favouring ^2E_g and the other $^4T_{2g}$ as the immediate precursor of reaction. Edelson and Plane (8) in 1959 were first to suggest that the ^2E_g was probably the precursor in the photoaquation of $[Cr(NH_3)_5(H_2O)]^{3+}$ and $[Cr(NH_3)_6]^{3+}$. They later suggested an explanation for the observation that aquation quantum yields (ϕ_a) increase with increasing ΔE (12), the energy difference between the maxima of the absorptions ($^4T_{2g} \leftarrow {}^4A_{2g}$)

and ($^2E_g \leftarrow {}^4A_{2g}$) (Fig. 5). They postulated a thermal back reaction from the ^2E_g to the $^4T_{2g}$ level, thus shortening the lifetime of ^2E_g and decreasing its inherent reactivity. For most Cr(III) complexes the zeroth level of $^4T_{2g}$ is higher in energy than the zeroth level of ^2E_g so that as Δ increases the separation between the zeroth levels of ^2E_g and $^4T_{2g}$ increases so that the thermal back reaction would be less efficient and thus the inherent reactivity of ^2E_g would increase. Generally ΔE varies with Δ. This increase of ϕ_a with increasing Δ and ΔE will henceforth be referred to as the ΔE rule.

Schläfer in 1965 (9) supported the views of Edelson and Plane and suggested that the lifetime of the quartet states was too short for chemical reaction to occur. He estimated that the excited quartet states have an average radiative lifetime of about 10^{-6} to 10^{-7} sec. vs. about 10^{-3} sec. for the doublet (^2E_g) state.

Adamson (10) has argued that there is no real reason why the $^4T_{2g}$ state cannot be the reactive intermediate, especially for the non-O_h complexes. He argues that the transition $^4T_{2g} \leftarrow {}^4A_{2g}$ places an electron in an antibonding orbital on the axis having the weakest average ligand field strength, thus explaining the lability of that axis observed in previous studies (4). He argues further that in the cases where spectrospecificity of the ratio of the reaction modes have been observed, at least two routes for aquation are required.

Porter (11) has very recently observed that quenching of the ^2E_g state of $[Cr(NH_3)_2(SCN)_4]^-$ by $[Cr(CN)_6]^{3-}$ results in $\phi_a(SCN^-)$ being

reduced to only about one-half the unquenched value. He interprets this as evidence that at least half of the photochemistry goes through the $^4T_{2g}$ state. He adds that if $^4T_{2g}$ and ^2E_g exist in thermal equilibrium at room temperature it is possible that all of the photochemistry goes through the $^4T_{2g}$ state.

D. The ΔE Rule and Adamson's Rules

A good deal of systematization has been given to the observed photochemical reactions of Cr(III) by two empirical rules.

a. The ΔE Rule (discussed previously on page 21)

The following series of ammine complexes was used by Edelson and Plane (12) to illustrate the ΔE rule. NH_3 is a stronger field ligand than H_2O so the average ligand field strength decreases down the list as does ϕ_a for ammonia aquation.

Complex	ϕ_a
$[Cr(NH_3)_6]^{3+}$	0.29
$[Cr(NH_3)_5(H_2O)]^{3+}$	0.17
$[Cr(NH_3)_4(H_2O)_2]^{3+}$	0.15
$[Cr(NH_3)_3(H_2O)_3]^{3+}$	0.02
$[Cr(NH_3)_2(H_2O)_4]^{3+}$	0.002

Most pure O_h complexes also generally follow the ΔE rule.

b. Adamson's Rules for non-O_h Complexes (4)

"Rule 1. Consider the six ligands to lie in pairs at the ends of three mutually perpendicular axes. That axis having the smallest

average crystal field will be the one labilized, and the total quantum yield will be about that for an O_h complex of the same average field.

Rule 2. If the labilized axis contains two different ligands, then the ligand of greater field strength preferentially aquates. This may be a type of trans effect.

Rule 3. The discrimination implied by rules 1 and 2 will occur to a greater extent if it is the L_1 ($^4T_{2g} \leftarrow {}^4A_{2g}$) rather than the L_2 ($^4T_{1g} \leftarrow {}^4A_{2g}$) band that is irradiated."

V. STATEMENT OF THE PROBLEM

Use of the aquo-ammine series of Cr(III) complexes on which to base the ΔE Rule has been criticized on the basis that the quantum yields for water exchange are not known and it is not strictly valid to compare aquation quantum yields of complexes unless all modes of aquation are considered.

Adamson's Rules are qualitatively consistent with the known photochemistry of Cr(III) complexes but the quantitative predictions appear to conflict with the ΔE Rule in that Adamson's Rules consider the average field strength of the two ligands on the labilized axis to determine the magnitude of ϕ_a. The ΔE Rule, on the other hand, considers the average field strength of all six ligands to determine the magnitude of ϕ_a.

The complexes in this work were chosen to test the ΔE Rule and Adamson's Rules.

The series of complexes:

$$[Cr(en)_3]^{3+}$$
$$[Cr(en)_2ox]^{+}$$
$$[Cr\ en(ox)_2]^{-}$$
$$[Cr(ox)_3]^{3-}$$

which displays a decrease in average ligand field strength as one goes from $[Cr(en)_3]^{3+}$ to $[Cr(ox)_3]^{3-}$, was expected to test the ΔE Rule. It

was known that $[Cr(en)_3]^{3+}$ has $\phi_a = 0.37$ (13) for the reaction

$$[Cr(en)_3]^{3+} \xrightarrow{h\nu} [Cr(enH)en_2(H_2O)]^{4+} \qquad (12)$$

and $[Cr(ox)_3]^{3-}$ has $\phi_a < 1 \times 10^{-3}$ in the visible region (14). The intermediate complexes were expected to show ϕ_a's somewhere between the two extremes. It was thought that the ϕ_a for both possible modes of aquation for $[Cr(en)_2ox]^{+}$ and $[Cr\ en(ox)_2]^{-}$ could be measured allowing unambiguous ordering of the ϕ_a for the complete series.

In addition these complexes could be used to test Adamson's Rules which predict ethylenediamine aquation for $[Cr(en)_2ox]^{+}$ and oxalate aquation for $[Cr\ en(ox)_2]^{-}$ (Fig. 6).

The pair of complexes cis and trans-$[Cr(en)_2Cl_2]^{+}$ were chosen as a further test of Adamson's Rules. Although the overall ligand field strength is the same for both complexes, Adamson's Rules predict different modes of photolysis. Since Cl^{-} is a much weaker field ligand than ethylenediamine the predicted modes are ethylenediamine aquation for the cis isomer and Cl^{-} aquation for the trans isomer (Fig. 6).

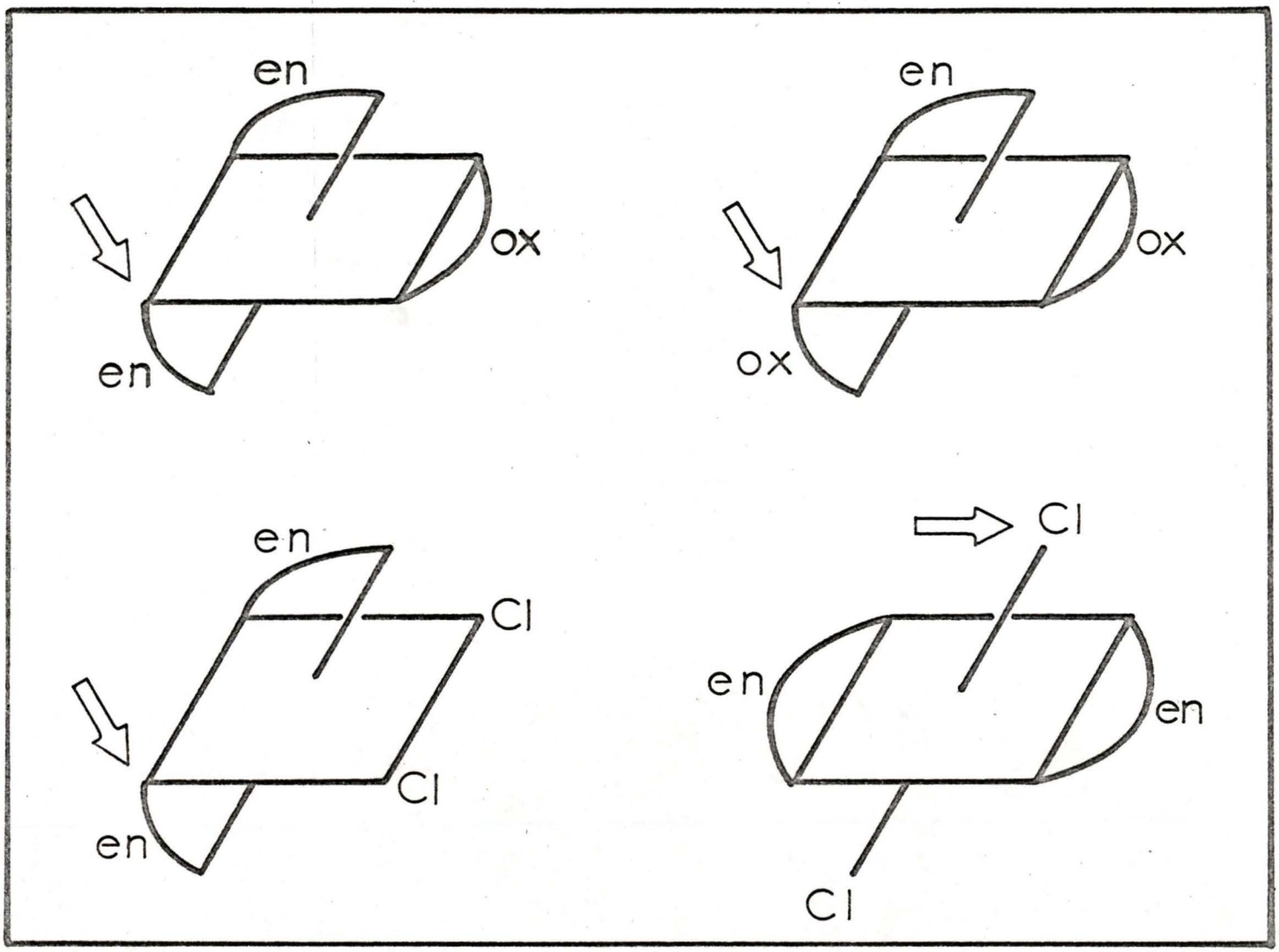

FIGURE 6. Adamson's Rules for cis and trans $[Cr(en)_2Cl_2]^+$, $[Cr(en)_2ox]^+$, and $[Cr(en)(ox)_2]^-$.
(Arrows indicate the Labilized positions)

VI. EXPERIMENTAL

A. Preparations

1. $K[Cr\ en(ox)_2]\cdot 2H_2O$ was prepared according to the method of Schläfer (17) with the following modification. Sixteen gm. of ethylenediamine was heated with 100 gm. of $K_3[Cr(ox)_3]\cdot 3H_2O$ in 100 ml. of water rather than 1000 ml. of water. The product crystallized from the solution on cooling after the $[Cr(en)_2ox]$ $[Cr\ en(ox)_2]$ double salt had been filtered off. The $K[Cr\ en(ox)_2]\cdot 2H_2O$ was recrystallized by dissolving in the minimum amount of 50°C water, filtering and cooling the solution rapidly on ice.

	Theoretical	Found
%Cr	14.3	14.8
%C	19.8	20.5
%H	3.3	3.2
%N	7.7	7.9

2. $[Cr(en)_2ox]Cl\cdot H_2O$ was prepared according to the method of Bushra and Johnson (18) except that the reaction of $[Cr(en)_2ox]$ $[Cr\ en(ox)_2]$ with HCl was done at 0°C. The product was recrystallized by dissolving in the minimum amount of 60°C water, filtering and cooling rapidly on ice.

	Theoretical	Found
%Cr	16.6	16.4
%C	23.0	23.3
%H	5.8	6.2
%N	17.8	17.8

3. trans-$[Cr(en)_2Cl_2]Cl$ was prepared as described in ref. 19 It was found that the Cl_2 had to bubble through the $[Cr(en)_2(SCN)_2]SCN$ slurry overnight for good yields.

4. cis-$[Cr(en)_2Cl_2]Cl$ was prepared as described in ref. 20

5. trans-$[Cr(en)_2Cl_2]NO_3$ was prepared by adding conc. nitric acid to a solution of trans-$[Cr(en)_2Cl_2]Cl$ and cooling on ice. The product begins to separate immediately upon the addition of the nitric acid.

%Cr Theoretical 17.0 Found 16.9

6. cis-$[Cr(en)_2Cl_2]NO_3$ was prepared from cis-$[Cr(en)_2Cl_2]Cl$ by dissolving the latter in the minimum amount of water at room temperature, adding a large excess of NH_4NO_3 and cooling on ice.

%Cr Theoretical 17.0 Found 16.8

There is some disagreement in the literature about the number of waters of hydration in $[Cr(en)_2ox]Cl\cdot H_2O$ and $K[Cr\ en(ox)_2]\cdot 2H_2O$, so thermogravimetric analysis was used to confirm the number of waters of hydration in each complex. Results obtained using a Cahn RG Electrobalance coupled with an F. and M. 240 Temperature Programmer are illustrated in Fig. 7 . The formulae given above were found to be correct.

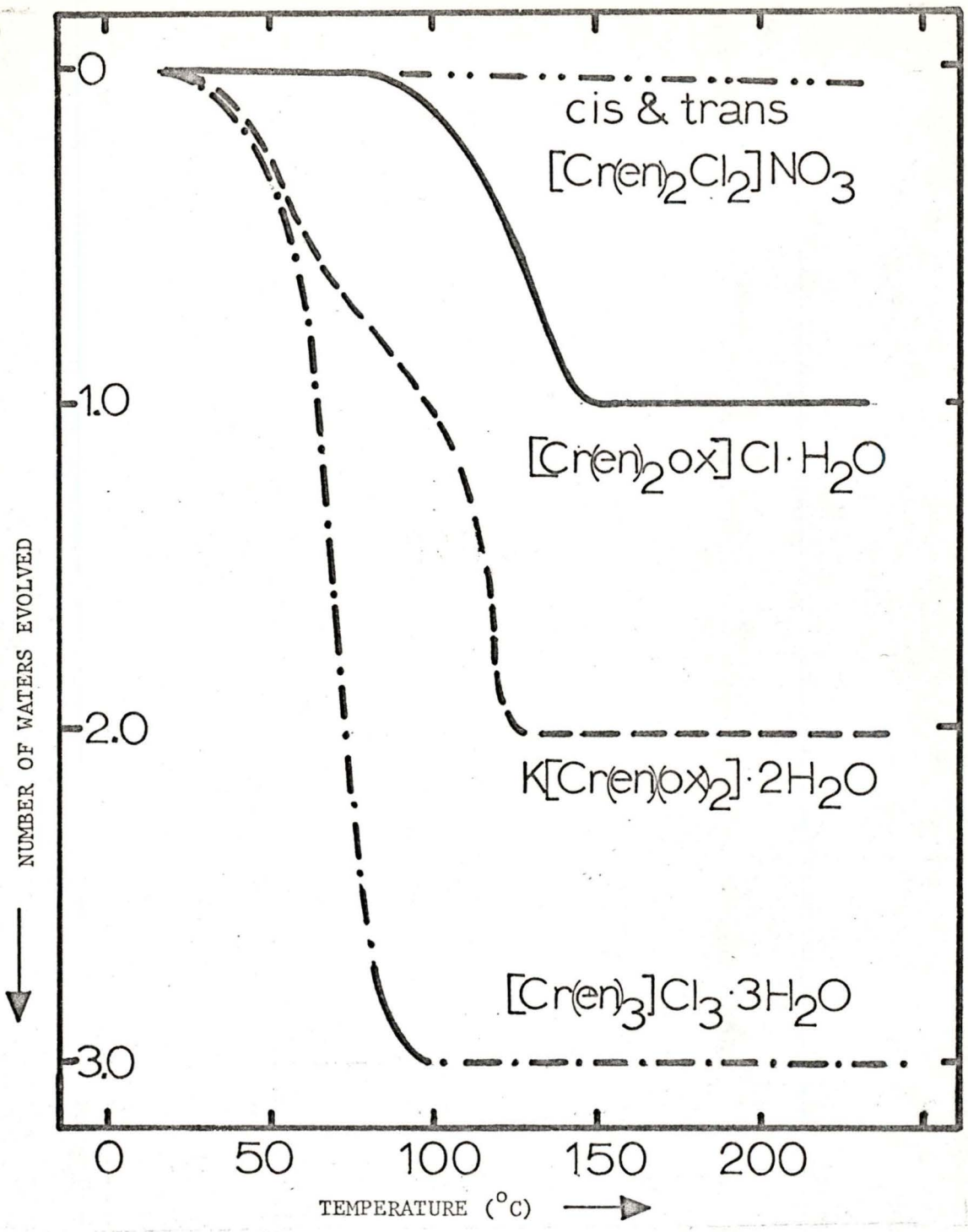

FIGURE 7. Thermal-gravimetric Analysis of:

—···— cis and trans $[Cr(en)_2Cl_2]NO_3$

——— $[Cr(en)_2ox]Cl\cdot H_2O$

– – – – $K[Cr(en)(ox)_2]\cdot 2H_2O$

—·— $[Cr(en)_3]Cl_3\cdot 3H_2O$

B. Measurement of Quantum Yields

1. Photolysis Apparatus

Fig. 8 shows schematically the photolysis apparatus used to measure quantum yields. Details of the equipment used are given in the legend to Fig. 8 . The quartz lens focussed the light from (A) onto a point just behind the photolysis cell. This ensured that the beam was slightly convergent as it passed through the cell and together with edge masks on the cell eliminated the possibility of any anomalous cell wall effects of the type reported by Lee and Seliger (21).

The quartz window at (E) reflected a constant, wavelength independent fraction of about 8% of the filtered beam onto the photocell at (J) so that the intensity of the lamp could be monitored continuously.

The constant temperature bath had a double quartz window at (F) which was purged with dry air during the $0^{o}C$ runs to eliminate misting on the window surface.

A cell holder was built at (G) so that the photolysis cell could be reproducibly positioned in the light beam.

Narrow band interference filters (Filtraflex B-20 - Rolyn Corp.) were used for all the quantitative runs. The measured band widths at

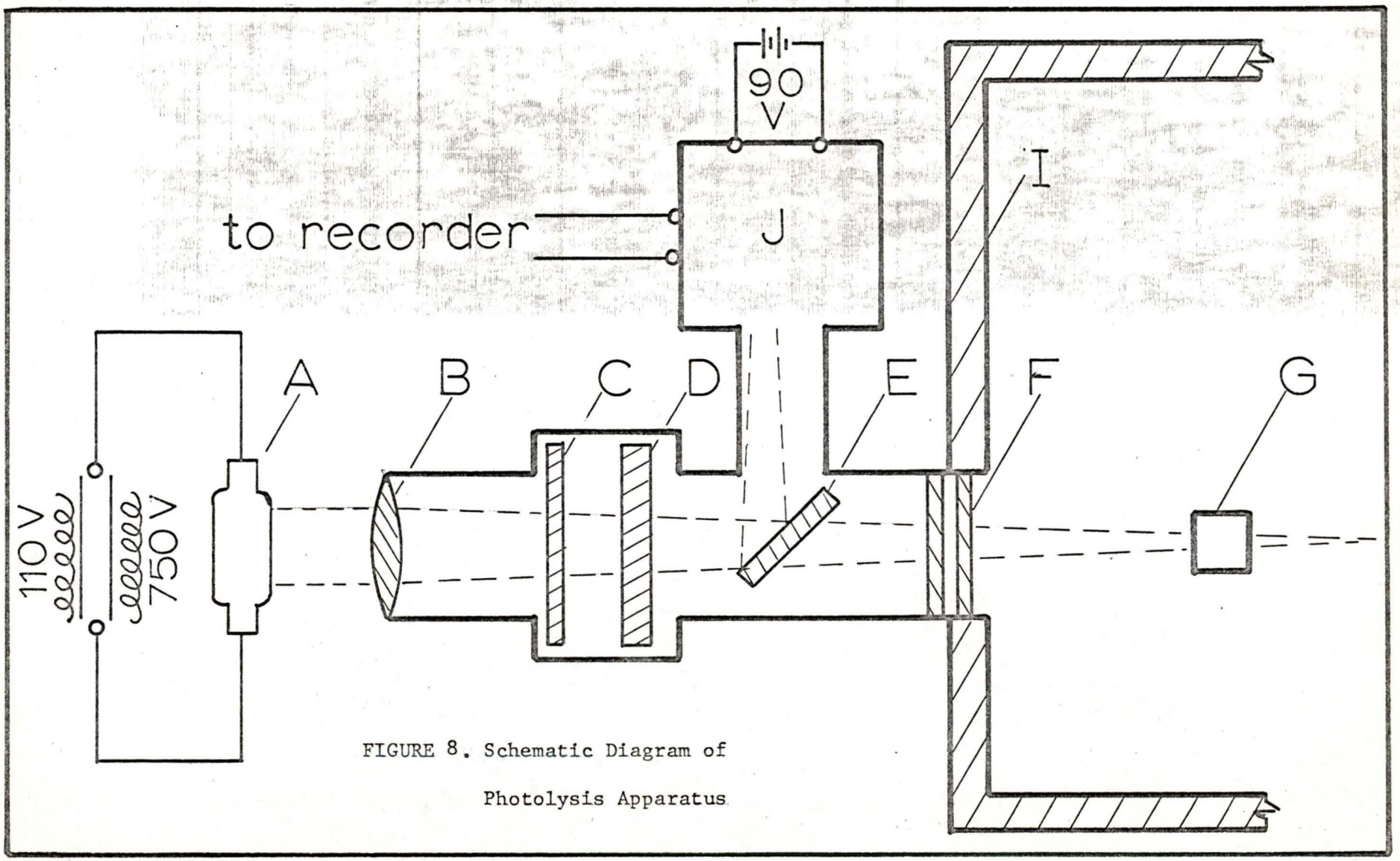

FIGURE 8. Schematic Diagram of Photolysis Apparatus

LEGEND TO FIGURE 8

A. Light source - AH6-1-B high pressure mercury capillary lamp, P.E.K. Laboratories Inc.

B. Quartz lense.

C. Heat reflecting filter - Calflex C, Rolyn Corp.

D. Interference filter - Filtraflex B-20, Rolyn Corp.

E. Quartz window.

F. Double quartz window.

G. Position of photolysis cell.

I. Constant temperature bath.

J. Photocell.

half height of the filters were:

Nominal Wavelength (n.m.)	Band Widths (n.m.)
400	5
424	9
540	7
565	6

For the preparative runs a wide band colour filter (CS-496) was used to allow more light to reach the sample.

The light flux reaching the photolysis cell was calibrated by chemical actinometry using solutions of $K[Cr(NH_3)_2(NCS)_4]$ (22).

2. Measurement of Light Intensity

3 ml. of a 2.0×10^{-2} M aqueous solution of $K[Cr(NH_3)_2(NCS)_4]$ at its natural pH was pipetted into the photolysis cell positioned in the cell holder. The shutter was opened to admit the light simultaneously with the starting of a timer. The output of the photocell measuring the reflected part of the light beam was followed by a millivolt recorder for the entire actinometer run. At the end of the run the shutter was closed simultaneously with the stopping of the timer. The actinometer solution was analyzed for SCN^- as described by Adamson and Wegner (22). All actinometer runs were done at 23°C.

The time of photolysis, concentration of SCN^- and the quantum yield

of the actinometer at the wavelength of irradiation (22) were used to calculate the flux of light reaching the photolysis cell in Einstein $sec.^{-1}$. The millivolt reading on the recorder then allowed the establishment of a conversion factor for light flux in terms of Einstein $sec.^{-1}$ $millivolts^{-1}$. At least two actinometer runs were made before and after each set of quantum yield determinations at a particular wavelength.

This procedure for measuring the light fluxes was necessitated because the ϕ_a of $K[Cr(NH_3)_2(NCS)_4]$ had been shown by Adamson and Wegner (22) to be somewhat dependent on temperature and had not been calibrated at the temperatures used for all the runs in this work. The above procedure allowed the calibration of the photocell to be made with the chemical actinometer at 23°C (at which temperature ϕ_a was precisely known) and subsequent photolysis runs to be made at any desired temperature with the light flux measurements made independent of the photolysis bath temperature. Another advantage of this procedure was that the light fluxes could be measured continuously and corrections made for any small variations of lamp output during the run.

3. The Photolysis Cell

The photolysis cell (Fig. 9) was a modified 1 cm. x 1 cm. glass spectrophotometer cell. The cell was designed to continuously follow changes in Cl^- or H^+ concentrations. Fig. 9 shows the cell set up for Cl^- measurements.

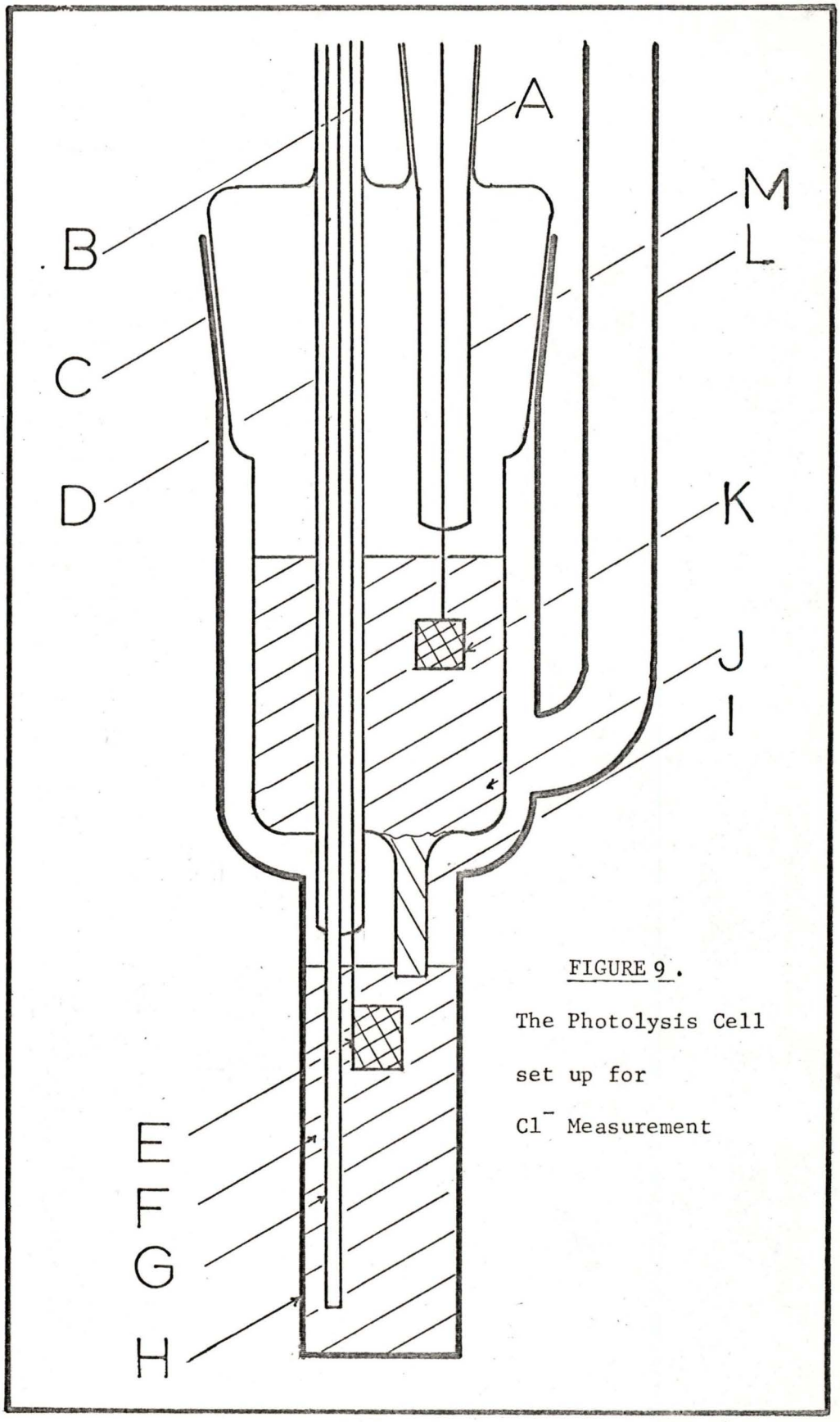

FIGURE 9.

The Photolysis Cell set up for Cl^- Measurement

LEGEND TO FIGURE 9

A. B-10/19 standard taper joint.

B. Silver wire.

C. B-19/26 standard taper joint.

D. 2mm. I.D. glass tubing.

E. 10 mm. x 7.5 mm. Ag/AgCl measuring electrode.

F. Sample solution.

G. Polyethylene tubing for N_2 bubbling.

H. 1 cm. x 1 cm. glass spectrophotometer cell.

I. Agar plug saturated with NH_4NO_3.

J. Reference KCl solution (1.0×10^{-2} M).

K. 10 mm. x 7.5 mm. Ag/AgCl reference electrode.

L. Sidearm for sample delivery.

M. 2 mm. I.D. glass tubing.

The Cl^- measuring cell was a concentration cell without transference and gave reproducible readings for several weeks when stored in the dark. The internal reference cell contained 1.00×10^{-2} M KCl. The silver reference and measuring electrodes were coated with a layer of AgCl by electrolysis in a KCl solution. The measuring electrode was calibrated from 1.00×10^{-4} to 2.00×10^{-3} M in Cl^- (Fig. 10). Wet nitrogen was bubbled through the reaction solutions to ensure good mixing throughout the runs. The front face of the cell was masked to avoid light falling on the edges of the cell or on the Ag/AgCl measuring electrode.

It was observed that exposure of the Ag/AgCl measuring electrode to the light beam during photolysis caused an immediate decrease in potential readings of several millivolts. The potential increased by an equivalent amount when the light was shut off. This phenomenon was not investigated further. Masking the cell to protect the electrode from light exposure successfully eliminated the problem.

4. Photolysis Runs

a. Instrumentation

Cl^- measurements were made by coupling the Ag/AgCl electrode to an I.L. Model 205 pH meter. pH measurements were made using a Fisher Microprobe combination electrode in place of the Ag/AgCl electrode. A Metrohm Compensator E 388 pH meter was used for pH measurements.

b. Procedure

A solution of the desired complex concentration and pH was made up

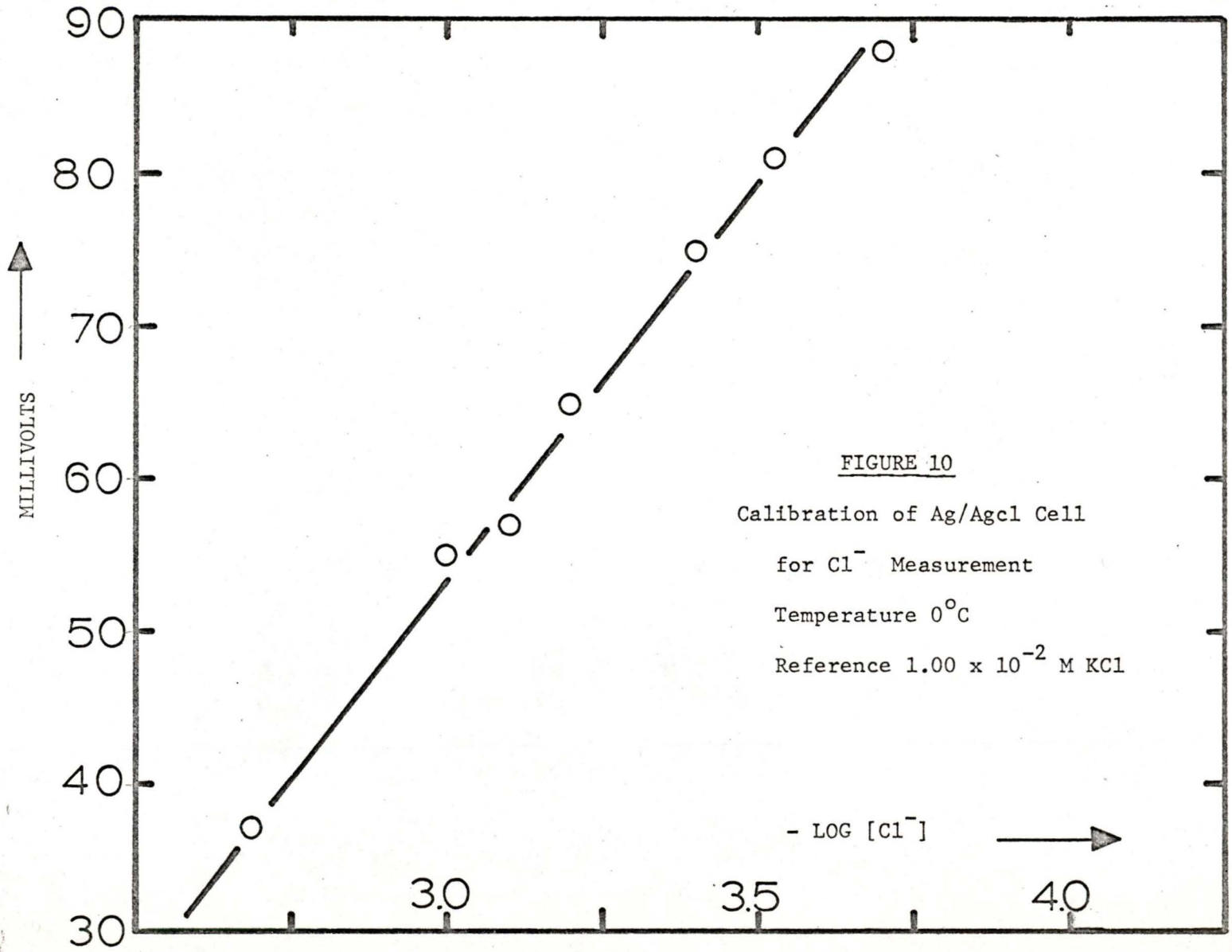

FIGURE 10

Calibration of Ag/Agcl Cell

for Cl^- Measurement

Temperature $0^{\circ}C$

Reference 1.00×10^{-2} M KCl

in semi-darkness using solutions and glassware that had been equilibrated at the run temperature. The cell was placed in position in the constant temperature bath and allowed to come to temperature equilibrium. Sufficient of the reaction solution was pipetted into the cell through the side arm (3.0 ml. for Cl^- runs and 5.0 ml. for pH runs). Potential or pH readings were taken with the shutter closed until it was apparent that the solution and electrode had reached thermal equilibrium. The dark reaction of the complex was then followed for a short time by taking potential or pH readings at convenient intervals. The shutter was then opened and the photochemical reaction followed. After about 5% of the complex had reacted the shutter was closed and the post photolysis dark reaction followed for a short time. Typical concentration vs. time curves for the photolysis runs are illustrated in Fig. 11, a, b, c, d.

c. Conditions

All photolysis runs were made at pH 3.0. For the cis and trans $[Cr(en)_2Cl_2]^+$ runs the solutions were 5.00×10^{-3}M in complex and 1.00×10^{-3}M in $HClO_4$. The ionic strength was adjusted to 1.0×10^{-2} with $KClO_4$. For the $[Cr(en)_2ox]^+$ and $[Cr\ en(ox)_2]^-$ runs the solutions were 1.0×10^{-2}M in complex and 1.0×10^{-3}M in HCl. The ionic strength was adjusted to 1.0×10^{-1} with KCl.

5. Calculation of the Quantum Yield

A number of approximations have been made in the following calculation scheme. These are discussed more fully and shown to be justified in the Discussion of Errors Section.

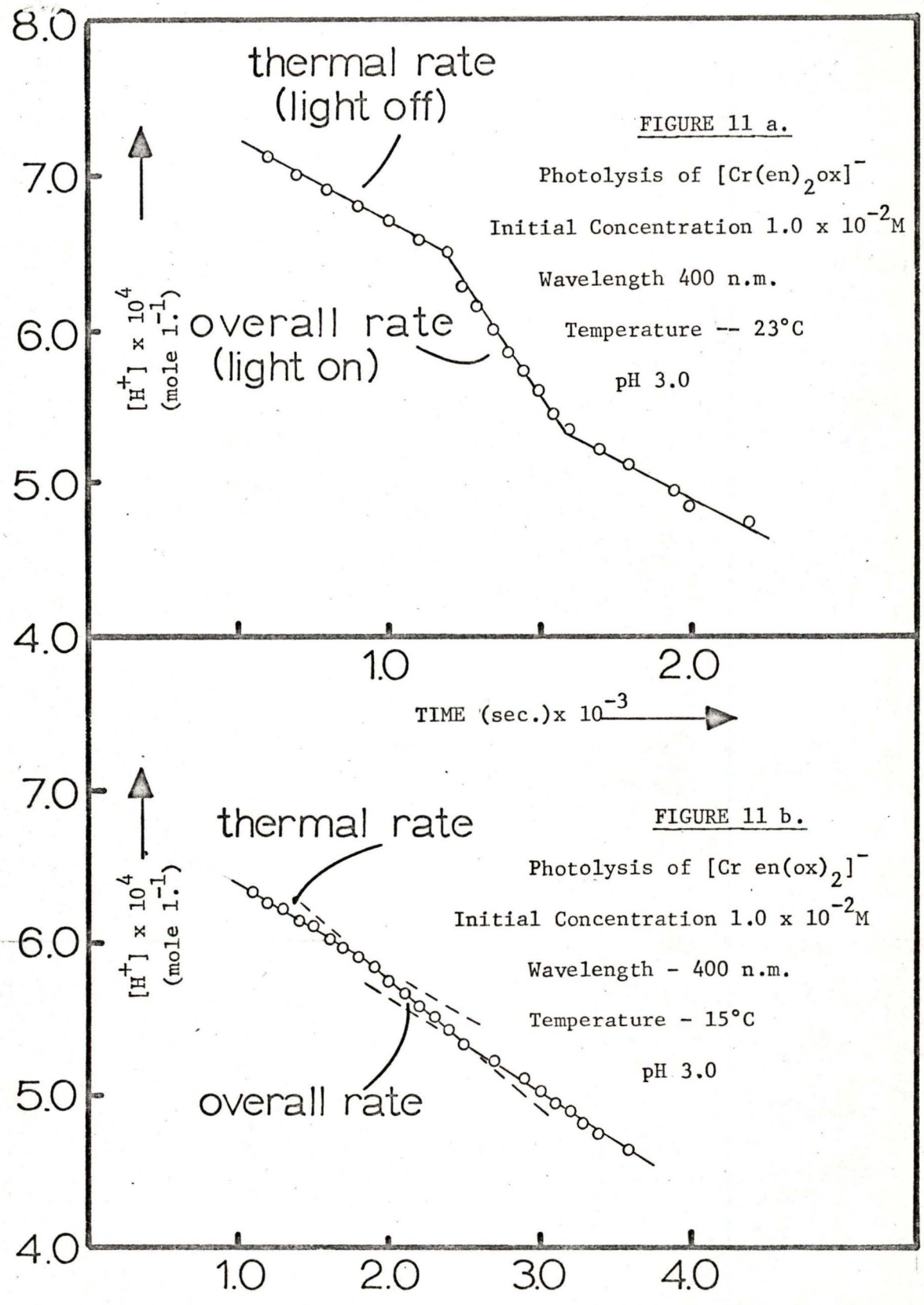

FIGURE 11 a.

Photolysis of $[Cr(en)_2ox]^-$

Initial Concentration 1.0×10^{-2}M

Wavelength 400 n.m.

Temperature -- 23°C

pH 3.0

FIGURE 11 b.

Photolysis of $[Cr\ en(ox)_2]^-$

Initial Concentration 1.0×10^{-2}M

Wavelength - 400 n.m.

Temperature - 15°C

pH 3.0

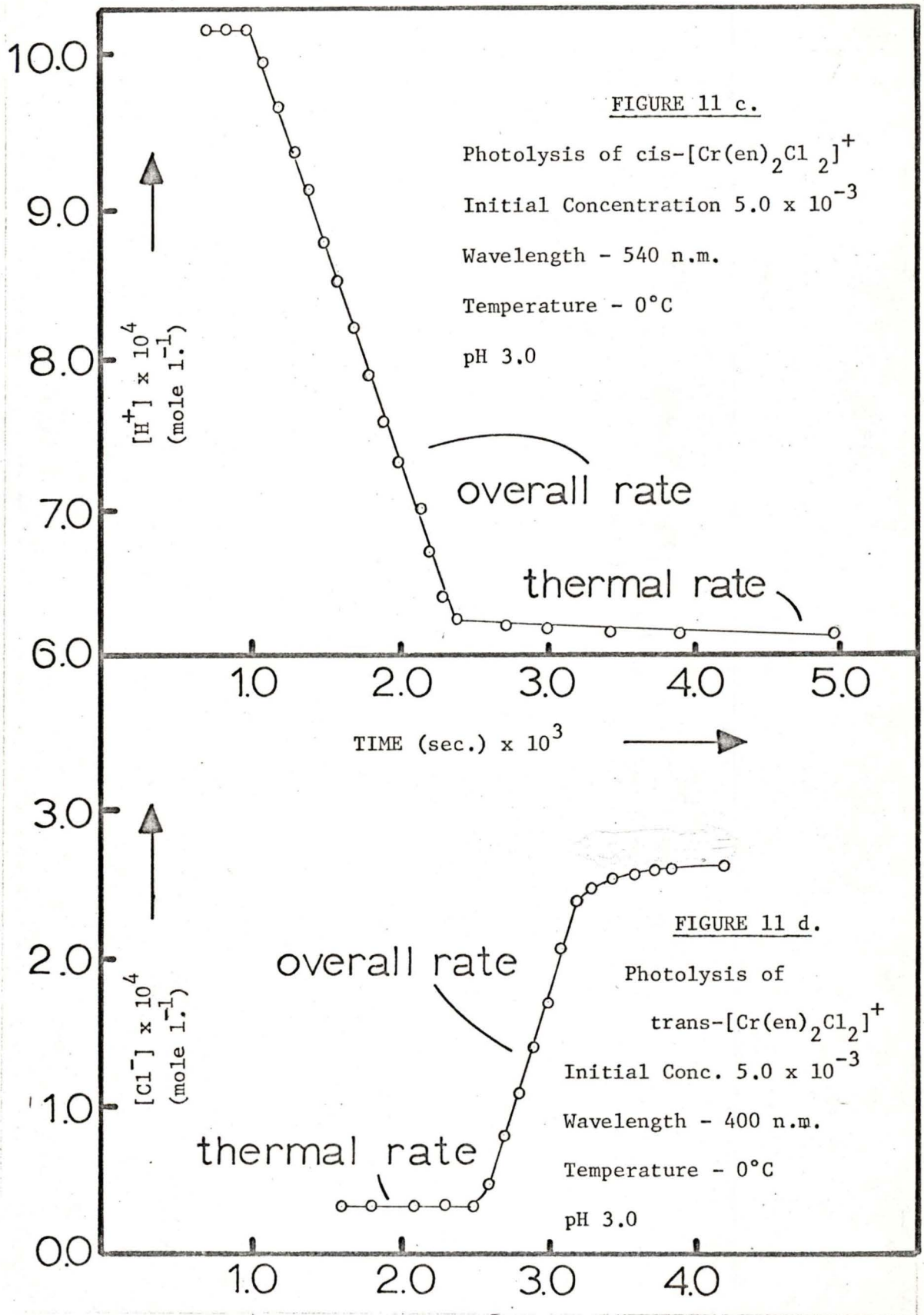

FIGURE 11 c.

Photolysis of cis-$[Cr(en)_2Cl_2]^+$

Initial Concentration 5.0×10^{-3}

Wavelength - 540 n.m.

Temperature - 0°C

pH 3.0

FIGURE 11 d.

Photolysis of

trans-$[Cr(en)_2Cl_2]^+$

Initial Conc. 5.0×10^{-3}

Wavelength - 400 n.m.

Temperature - 0°C

pH 3.0

The reaction rates were calculated directly from the slope of the concentration vs. time curves:

$$\text{rate (mole } l.^{-1} \text{ sec.}^{-1}) = \frac{\text{concentration change}}{\text{time}}$$

The photolysis rate was then separated from the accompanying thermal rate:

$$\text{photolysis rate (mole } l.^{-1} \text{ sec.}^{-1}) = \text{overall rate} - \text{thermal rate}$$

Multiplying this by the volume of the reaction solution gives the photolysis rate in moles sec.^{-1} . The average concentration of complex during the photolysis was calculated from the concentrations at the beginning and end of the photolysis. This value was used to calculate the average absorbance of the solution at the wavelength of photolysis. The intensity of the lamp had been previously calibrated and knowing the average absorbance of the solution the average intensity absorbed could be calculated:

$$\text{average intensity absorbed (Einstein sec.}^{-1}) = \text{lamp intensity} \times \% \text{ absorbance} \times 10^{-2}$$

(where % absorbance = 100 - % transmittance)

The quantum yield can now be calculated directly:

$$\text{quantum yield (moles Einstein}^{-1}) = \frac{\text{photolysis rate (moles sec.}^{-1})}{\text{average intensity absorbed (Einstein sec.}^{-1})}$$

Inner filter effects were found to be small compared to the uncertainties in the rates and were therefore not applied, except in the case of trans-$[Cr(en)_2Cl_2]^+$.

C. Ion Exchange Chromatography

Identification of monodentate ethylenediamine complexes and cis and trans isomers of the $[Cr(en)_2Cl_2]^+$ ion and its aquation products was done by separating the complex ions in the photolysis solutions using ion exchange chromatography and, where possible, measuring the visible absorption spectra of the separated complex ions.

All chromatography was done on a 1 cm. x 10 cm. jacketed column at 0^oC.

Table (1) shows the types of resins and eluents used for the various chromatographic separations.

Where quantitative results were required each fraction eluted from the column was analyzed for Cr(III).

D. Chromium Analysis

All Cr(III) analyses were made using an alkaline peroxide oxidation technique. The solution to be analyzed was made alkaline with aqueous ammonia and a small excess of H_2O_2 was added. The solution was heated on a steam bath for about twenty minutes, additonal aqueous ammonia was added to ensure alkalinity and the solution diluted to a known volume. The absorbance of the CrO_4^- formed was read at 373 n.m. and compared to a previously prepared calibration curve.

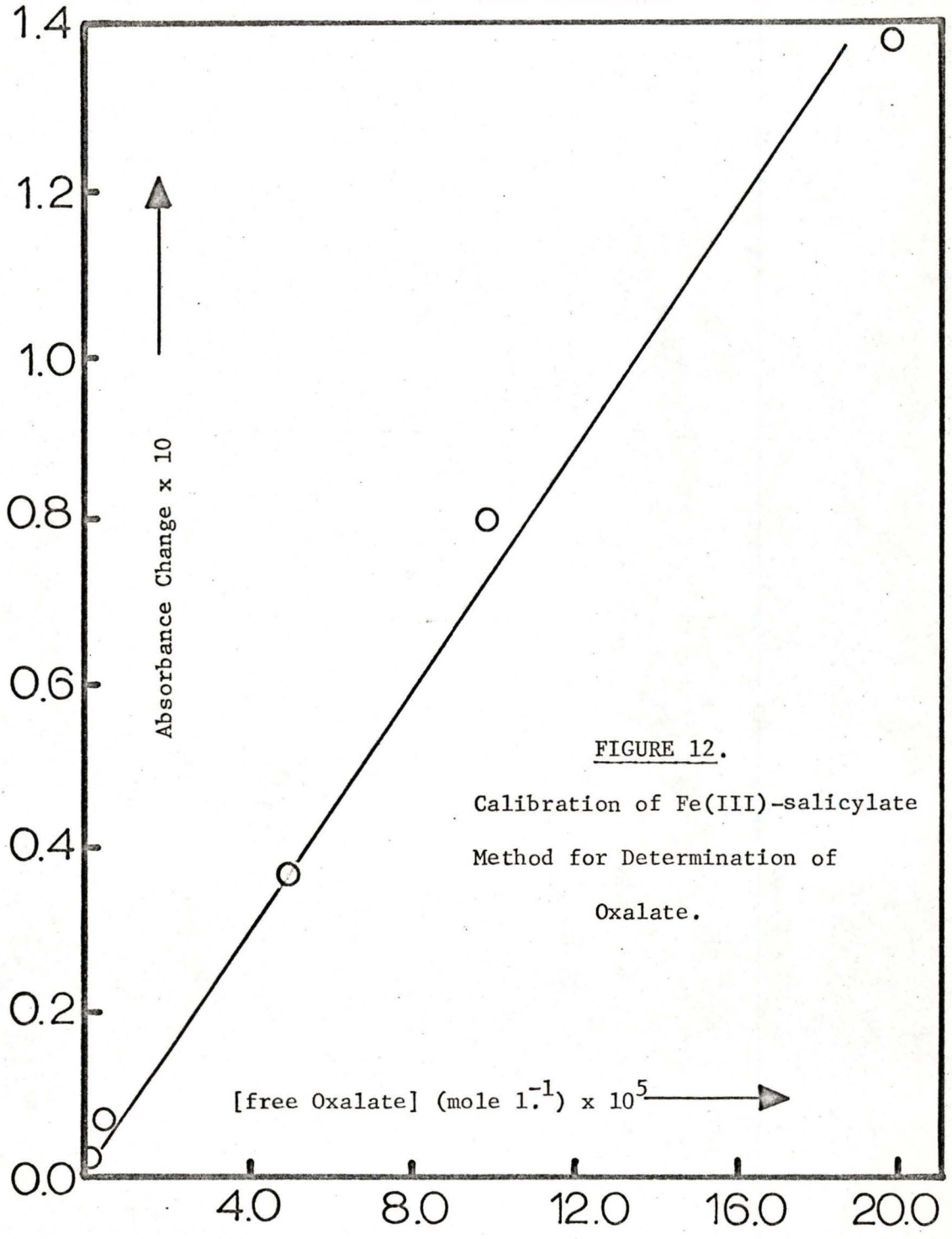

FIGURE 12.

Calibration of Fe(III)-salicylate Method for Determination of Oxalate.

E. Spectrophotometric Measurement of Thermal Rates

Thermal aquation rates of some of the photochemical reaction products were found by observing spectral changes at constant temperature. The complexes were separated from reaction solution by ion exchange chromatography and their spectral changes followed using a Unicam SP-700 U.V. - visible spectrophotometer equipped with a constant temperature cell compartment. The pH of the solution was determined by the eluent used in the chromatography and was about 2 or 3 depending on the complex. (See Discussion)

F. Oxalate Analysis

All analyses for free oxalate in the photolysis solutions were made using the method of Burriel-Marti et al (23) with the following modifications:

4 ml. of the Fe(III)-salicylate solution was pipetted into a 10 ml. volumetric flask and 3 ml. of the photolysis solution added. The solution was made up to 10 ml. and the absorbance read at 19,500 $cm.^{-1}$. The method was calibrated by adding 3 ml. aliquots of 1.0×10^{-2}M $K[Cr\ en(ox)_2]\cdot 2H_2O$ containing kown amounts of free oxalate. The calibration curve is displayed in Fig. 12.

VII. RESULTS

A. Photoaquation of $[Cr(en)_2ox]^+$

1. Thermal Reactions

No information about the thermal aquation reactions of $[Cr(en)_2ox]^+$ could be found in the literature. Spectral changes of an aqueous solution of $[Cr(en)_2ox]^+$ at pH 1.0 to 3.0 suggest a thermal aquation reaction of

$$[Cr(en)_2ox]^+ \xrightarrow{k_1} [Cr\ en(H_2O)_2ox]^+ \qquad (13)$$

k_1 was found to be about 0.6×10^{-5} sec.$^{-1}$ at 23°C by following the pH change during thermal reaction in the dark. Stable protonated, monodentate ethylenediamine intermediates have been identified in other systems (13), (24) and it is thought that the above reaction goes through the protonated monodentate ethylenediamine intermediate described below.

2. Identification of the Photolysis Products

Photolysis of $[Cr(en)_2ox]^+$ with visible light at pH 1.0 to 3.0 and at temperatures from 0°C to 23°C produced a change in solution colour from orange to red. Separation of the photolysis solution on a weak cation exchange resin (Table 1) at 0°C resulted in the isolation of a solution of a red complex which was observed to decompose thermally in acidic solution to give $[Cr\ en(H_2O)_2ox]^+$

$$[Cr(en)_2ox]^+ \xrightarrow{h\nu} [A] \xrightarrow{k_2} [Cr\ en(H_2O)_2ox]^+ \qquad (14)$$

where $k_2 \simeq 1 \rightarrow 5 \times 10^{-5}$ sec.$^{-1}$

The fact that $k_2 > k_1$ explained the absence of [A] in the thermal aquation of $[Cr(en)_2ox]^+$, as none was found by ion exchange separation of the thermal solutions.

The visible absorption spectrum of [A] showed peak maxima and extinction coefficients intermediate between those of $[Cr(en)_2ox]^+$ and $[Cr\ en(H_2O)_2ox]^+$ (Fig. 13). The spectrum of [A] was also determined by comparing the spectrum of a solution of $[Cr(en)_2ox]^+$ with the spectrum obtained from the same solution after 50% of the $[Cr(en)_2ox]^+$ had been decomposed by photolysis. The weighted spectrum of the starting material was subtracted out from the spectrum of the mixture to obtain the spectrum of the photolysis product. Although this type of analysis leaves itself open to errors incurred by secondary photolysis or thermal decomposition of the photolysis product the agreement between the measured and calculated spectrum of [A] is quite good (Fig. 13).

The spectrum of [A] was used to identify the complex in the following manner. Consider the series of spectra for cis-$[Cr(NH_3)_4(H_2O)_2]^{3+}$, $[Cr(NH_3)_3(H_2O)_3]^{3+}$, and cis-$[Cr(NH_3)_2(H_2O)_4]^{3+}$ (Fig. 14). If one considers only the atoms that are coordinated to the Cr(III) central ion, then the above amino-aquo series is entirely analogous to the series $[Cr(en)_2ox]^+$, $[Cr\ en(enH)(H_2O)ox]^{2+}$ and $[Cr\ en(H_2O)_2ox]^+$ in that the complexes have (4 nitrogens, 2 oxygens), (3-N,3-O) and (2-N,4-O) coordinating atoms respectively in each series. Comparing Fig.'s 13 and 14 shows that the spectral changes for the two

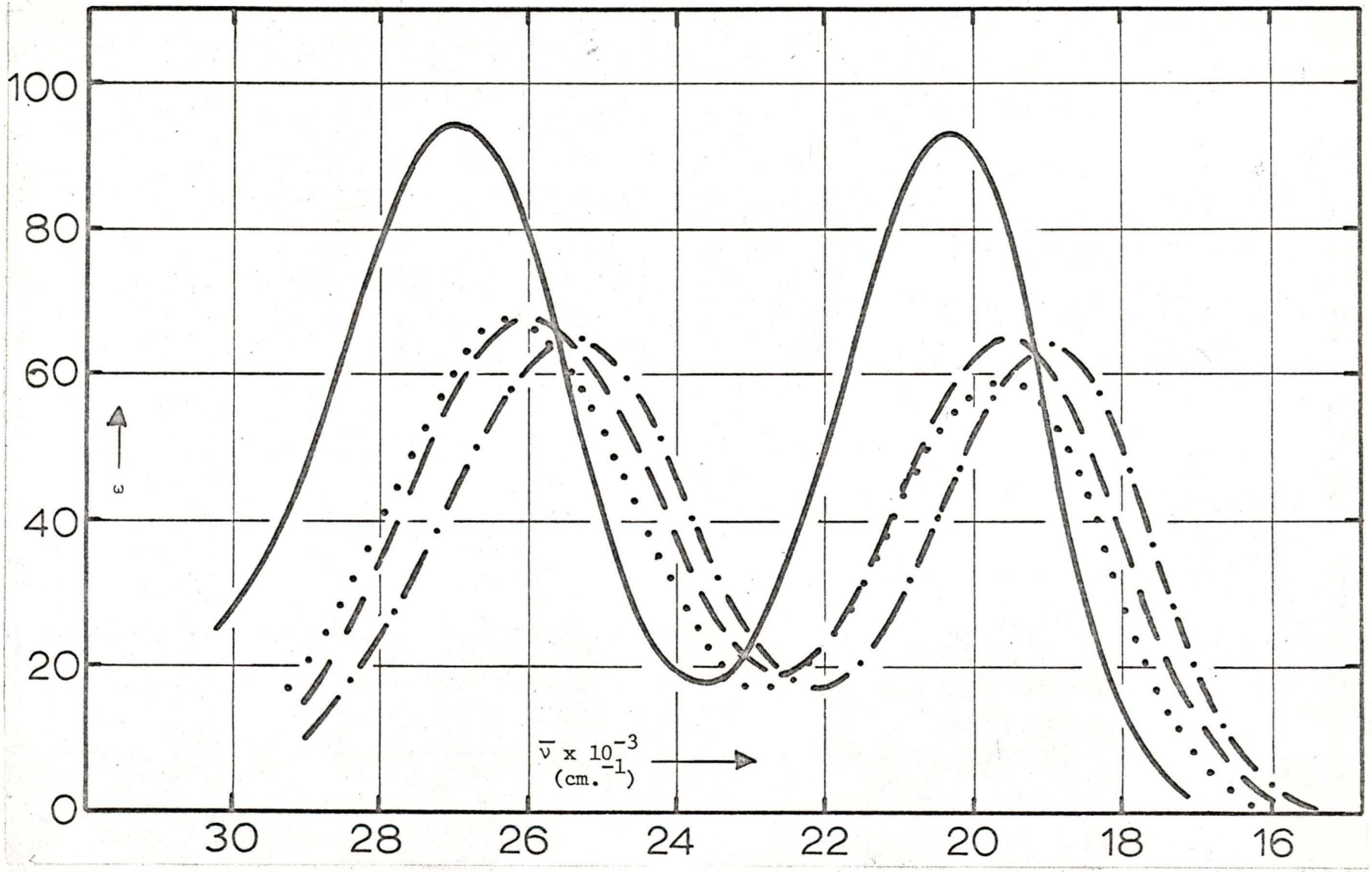

FIGURE 13. Visible Absorption Spectra of: ——— $[Cr(en)_2ox]^+$, – – – $[Cr\ en(enH)(H_2O)ox]^{2+}$, —·— $[Cr\ en(H_2O)_2ox]^+$, ····· $[Cr\ en(enH)(H_2O)ox]^{2+}$ (calculated).

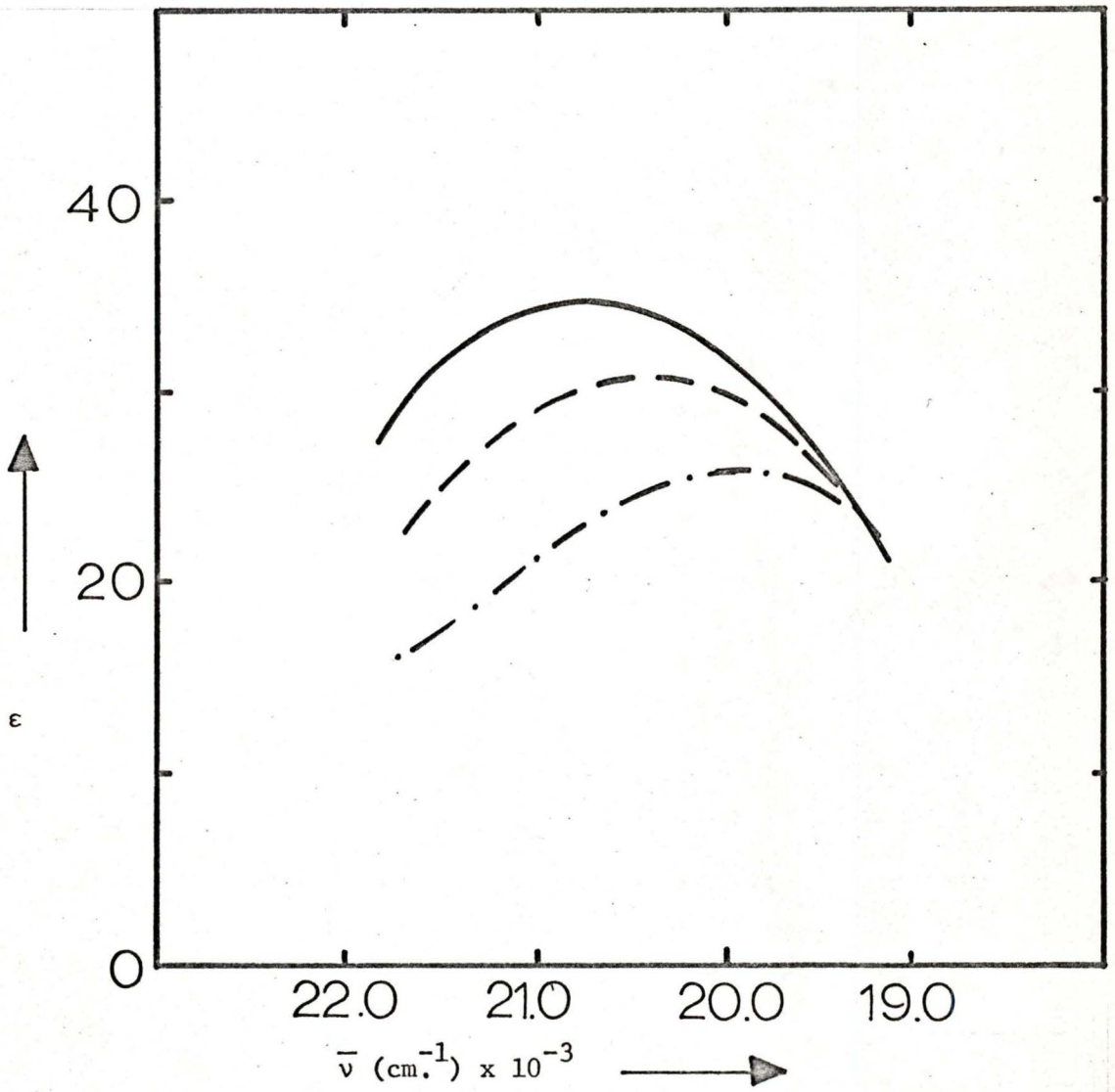

FIGURE 14. Absorption Spectra of:

——— $[Cr(NH_3)_4(H_2O)_2]^{3+}$

– – – $[Cr(NH_3)_3(H_2O)_3]^{3+}$

·—·— $[Cr(NH_3)_2(H_2O)_4]^{3+}$

Showing the Shift in Absorption Maximum on Succesive Replacement of NH_3 with H_2O. (Reproduced from ref. 8)

series are analogous with regard to the spectral shift of the peak maxima on exchanging a nitrogen for an oxygen. The foregoing is in agreement with ligand field theory prediction that replacement of a strong field ligand (N) with a weak field ligand (O) reduces Δ and thus shifts the d-d absorption bands to lower energies. In light of the theoretical predictions that a (3-N,3-O) complex should have d-d absorption band maxima between those of (4-N,2-O) and (2-N,4-O) complexes and the agreement of theory with the aquo-ammine series the photolysis product of $[Cr(en)_2ox]^+$ appears to have 3 nitrogen and 3 oxygen coordinating ligands.

The chromatographic behaviour suggested that the ionic charge of the photolysis product was higher than either $[Cr(en)_2ox]^+$ or $[Cr\ en(H_2O)_2ox]^+$. Coupled with the spectral evidence described above, identification of monodentate ethylenediamine complexes in other systems (13), (24) and the decomposition to $[Cr(en)(H_2O)_2ox]^+$ with H^+ consumption, this led to the assignment of the formula $[Cr\ en(enH)(H_2O)ox]^{2+}$ to the ion [A].

3. Quantum Yields

No free oxalate was found in the photolysis solution. The lower limit of sensitivity of the oxalate test allows $\phi_a(ox)$ to be no greater than 2×10^{-3}.

$\phi_a(en)$ for the reaction:

$$[Cr(en)_2ox]^+ \xrightarrow{h\nu} [Cr\ en(enH)(H_2O)ox]^{2+} \quad (15)$$

was found to be $(1.6 \pm .2) \times 10^{-1}$ at pH 3.0 (average of

six runs at two wavelengths and two temperatures - see Table 2). The limited precision of the data allows no conclusions to be drawn about possible temperature or wavelength dependence of ϕ_a(en). Kirk, Moss and Valentin (25) have measured ϕ_a(en) of $[Cr(en)_2ox]^+$ by following the spectral changes of a 1.0×10^{-2} M solution of the complex at pH 1.0 and 3°C. They found ϕ_a(en) to be about $(2.0 \pm .5) \times 10^{-1}$, in good agreement with the results obtained in this work by following pH changes.

B. Photoaquation of $[Cr\ en(ox)_2]^-$

1. Thermal Reactions

Schläfer et al found the following thermal reaction for $[Cr\ en(ox)_2]^-$ at pH 1.0 and 20°C

$$[Cr\ en(ox)_2]^- \xrightarrow{k_3} [X] \xrightarrow{k_4} cis\text{-}[Cr(H_2O)_2(ox)_2]^- \qquad (16)$$

where $k_3 \simeq 30 \times 10^{-5}$ sec.$^{-1}$

$k_4 = 1.0 \times 10^{-5}$ sec.$^{-1}$

They suggested that the intermediate (X) in equation 16 has the formula $cis\text{-}[Cr(enH)(H_2O)ox]^{\cdot}$.

2. Identification of Photolysis Products

It was apparent from this work that the initial product of photolysis in acidic aqueous solution was neither $cis\text{-}[Cr(H_2O)_2(ox)_2]^-$ or identical with (X). A reaction scheme such as the following is thought to occur

$$[Cr\ en(ox)_2] \xrightarrow{h\nu} [Y] \xrightarrow{k_4'} [Z] \xrightarrow{k_4} cis\text{-}[Cr(H_2O)_2(ox)_2]^- \qquad (17)$$

Separation on an anion exchange resin of an aqueous solution of $[Cr\ en(ox)_2]^-$ that had been photolyzed with visible light at 0^oC and pH 2.0 → 3.0 resulted in the elution of (Y), an apparently neutral complex from the column (Table 1).

The eluted complex (Y) underwent rapid spectral changes, described below, which resulted in the formation of a more stable complex (Z) that had a visible absorption spectrum intermediate between that of $[Cr\ en(ox)_2]^-$ and $[Cr(H_2O)_2(ox)_2]^-$. The visible absorption spectra of the three complexes are displayed in Figure 15.

Spectral changes due to thermal reaction of (Z) suggested ethylenediamine aquation with a rate of 0.9×10^{-5} sec.$^{-1}$ at 25^oC. Since (Z) has an aquation rate very close to that found by Schläfer et al for (X), as well as having a spectrum intermediate between that of the starting material and the cis-$[Cr(H_2O)_2(ox)_2]^-$ and a neutral charge it is likely that (Z) and (X) are the same complex and both have the formula $[Cr(enH)(H_2O)(ox)_2]^o$ as suggested by Schläfer et al.

Equation (17) can now be expanded to the following series of reactions:

$$[Cr\ en(ox)_2]^- \xrightarrow{h\nu} [Y] \qquad (18)$$

$$[Y] \xrightarrow{k_4'} \text{cis-}[Cr(enH)(H_2O)(ox)_2]^o \qquad (19)$$

$$\text{cis-}[Cr(enH)(H_2O)(ox)_2]^o \xrightarrow{k_4} \text{cis-}[Cr(H_2O)_2(ox)_2]^- + enH^+ \qquad (20)$$

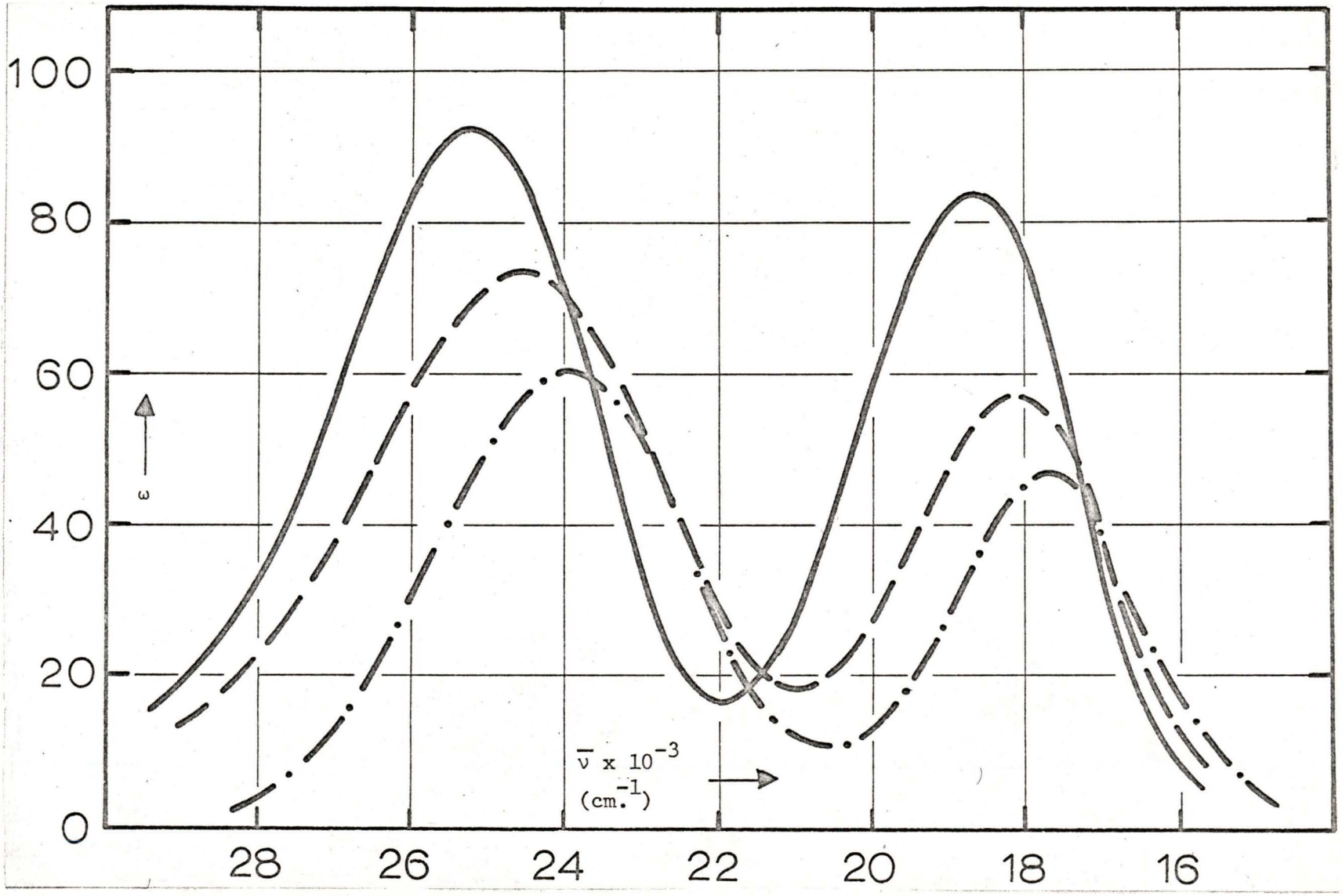

FIGURE 15. Visible Absorption Spectra of: —— $[Cr\ en(ox)_2]^-$, – – – $cis\text{-}[Cr(enH)(H_2O)(ox)_2]^\circ$ and —·—·— $cis\text{-}[Cr(H_2O)_2(ox)_2]^-$

k_4' was measured at 7×10^{-1} sec.$^{-1}$ at 0°C by following the spectral change in aqueous solution. During this change there was very little shift in the position of the peak maxima, but a 33% increase in extinction coefficient. This suggests that the reaction was not ethylenediamine aquation, since this is normally accompanied by a shift in the peak maxima to longer wavelengths. The direction and rate of the spectral change was similar to that of the trans to cis isomerization of $[Cr(H_2O)_2(ox)_2]^-$ and is thus considered to be a trans to cis isomerization of $[Cr(enH)(H_2O)(ox)_2]^o$ as shown in equation 19. Since $[Cr(H_2O)_2(ox)_2]^-$ and $[Cr(enH)(H_2O)(ox)_2]^o$ are very similar complexes it is not unreasonable to consider that their isomerization reactions might be similar. Fig. 16 shows an Arrhenius plot of the isomerization rates for the reaction:

$$\text{trans-}[Cr(ox)_2(H_2O)_2]^- \xrightarrow{H^+,\ H_2O} \text{cis-}[Cr(ox)_2(H_2O)_2]^- \qquad (21)$$

as found by Hamm et al (26). The points representing k_4' (equation 19) and k_4 (equation 20) are included to show that the rate constant k_4' is of the order required to fit the Arrhenius plot suggesting that the reaction (19) is similar to reaction (21). In contrast, the rate constant k_4 does not fit the Arrhenius plot. In fact, k_4' is only 3.5 times too large to exactly fit the plot while k_4 is 25 times too small. Since (Y) reacts with a rate similar to that of equation 21 to give cis-$[Cr(enH)(H_2O)(ox)_2]^o$ with very little shift in the absorption maxima, it is very likely that (Y) is trans-$[Cr(enH)(H_2O)(ox)_2]^o$ and the reaction (Y) → (Z) is a trans to cis isomerization.

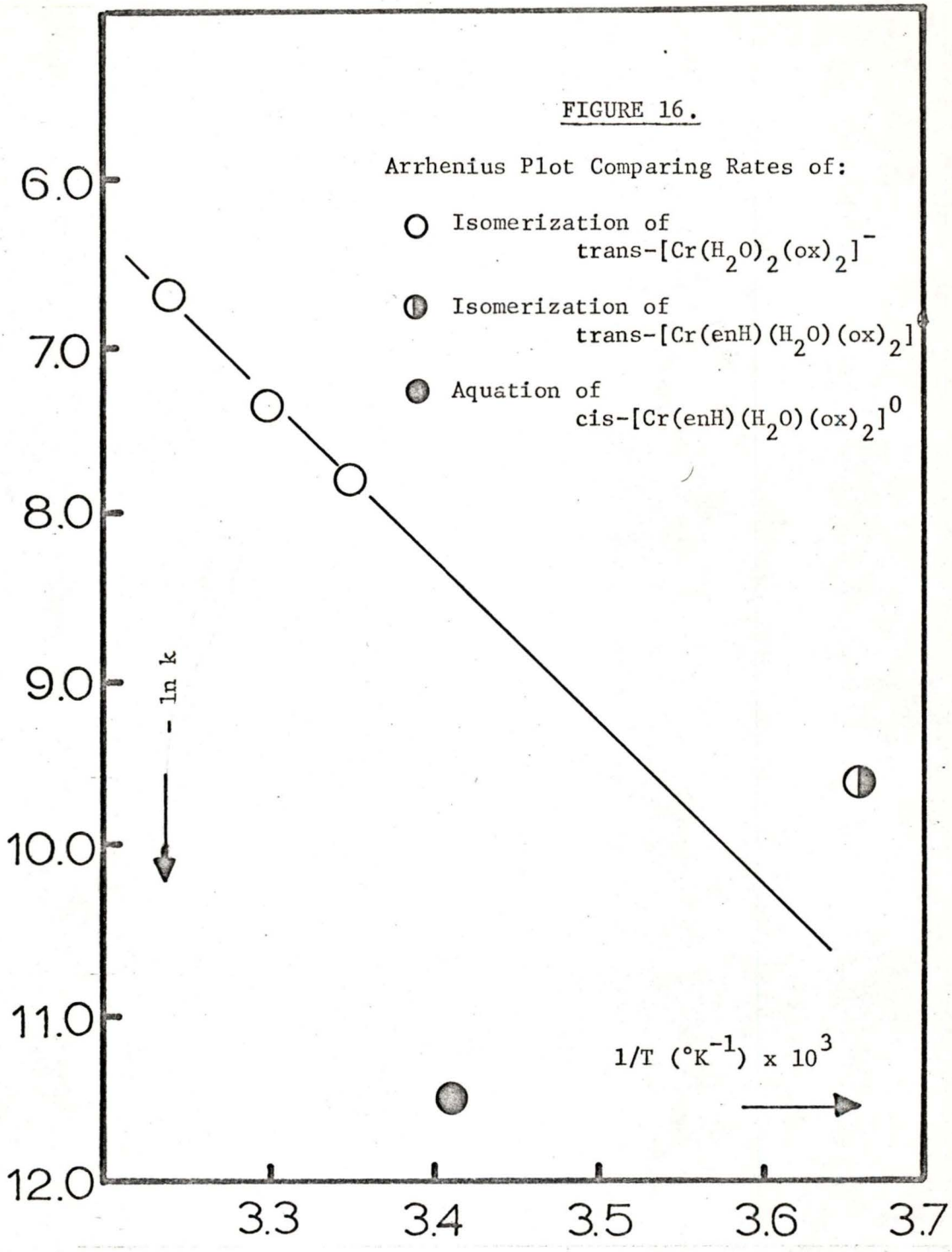

FIGURE 16.

Arrhenius Plot Comparing Rates of:

3. Quantum Yields

ϕ_a(en) for the reaction:

$$[Cr\ en(ox)_2]^- \xrightarrow{h\nu} [Cr(enH)(H_2O)ox_2]^o \qquad (22)$$

was found to be $(2.0 \pm .9) \times 10^{-2}$ at pH 3.0 and 15°C. No conclusions about possible wavelength or temperature dependence could be drawn (Table 2). Kirk, Moss and Valentin (25) found ϕ_a(en) to be $(1.5 \pm 1.0) \times 10^{-2}$ by following spectral changes of a 1.0×10^{-2} solution of $[Cr\ en(ox)_2]^-$ at 25°C and pH 1.0.

No free oxalate was found in the photolysis solution and an upper limit for ϕ_a(ox) is 1×10^{-3}.

C. Photoaquation of cis-$[Cr(en)_2Cl_2]^+$

1. Thermal Reactions

McDonald and Garner (27) have shown that Cl^- aquation is the preferred thermal reaction

$$cis\text{-}[Cr(en)_2Cl_2]^+ \xrightarrow{k_5} cis\text{-}[Cr(en)_2(H_2O)Cl]^{2+} + Cl^- \qquad (23)$$

where $k_5 = 111 \times 10^{-5}$ sec.$^{-1}$ at 35°C

They have also shown that the isomerization to trans-$[Cr(en)_2Cl_2]^+$ ($k = 0.5 \times 10^{-5}$ sec.$^{-1}$) and direct aquation to trans-$[Cr(en)_2Cl_2]^+$ ($k = 1 \times 10^{-5}$ sec.$^{-1}$ at 35°C) go very slowly relative to reaction 23.

2. Identification of Photolysis Products

Photolysis of an acidic aqueous solution of cis-$[Cr(en)_2Cl_2]^+$ at 0^oC and pH 3.0 with visible light resulted in a pH increase indicating ethylenediamine aquation. By analogy to the ethylenediamine-oxalate system a monodentate protonated ethylenediamine complex may be assumed to be formed as the major photolysis product, but the stereochemistry of the product is unknown.

$$cis\text{-}[Cr(en)_2Cl_2]^+ \xrightarrow{h\nu} [Cr(enH)(en)(H_2O)Cl_2]^{2+} \qquad (24)$$

Chloride photoaquation occurs, but much more slowly, and again the stereochemistry of the product is unknown.

$$cis\text{-}[Cr(en)_2Cl_2]^+ \xrightarrow{h\nu} [Cr(en)_2(H_2O)Cl]^{2+} + Cl^- \qquad (25)$$

Although the stereochemistry of the photolysis products has not been established, it should be possible to do this by ion exchange chromatography and arguments similar to those used in identifying the products in the ethylenediamine-oxalate system.

3. Quantum Yields

Photolysis of a 5.0×10^{-3} M aqueous solution of cis-$[Cr(en)_2Cl_2]^+$ at 0^oC and pH 3.0 with visible light gave $\phi_a(en) = (1.3 \pm .2) \times 10^{-1}$ for equation 24 and $\phi_a(Cl^-) = (1.0 \pm .5)$ to $(2.0 \pm 1.0) \times 10^{-2}$ for equation 25 (Table 2).

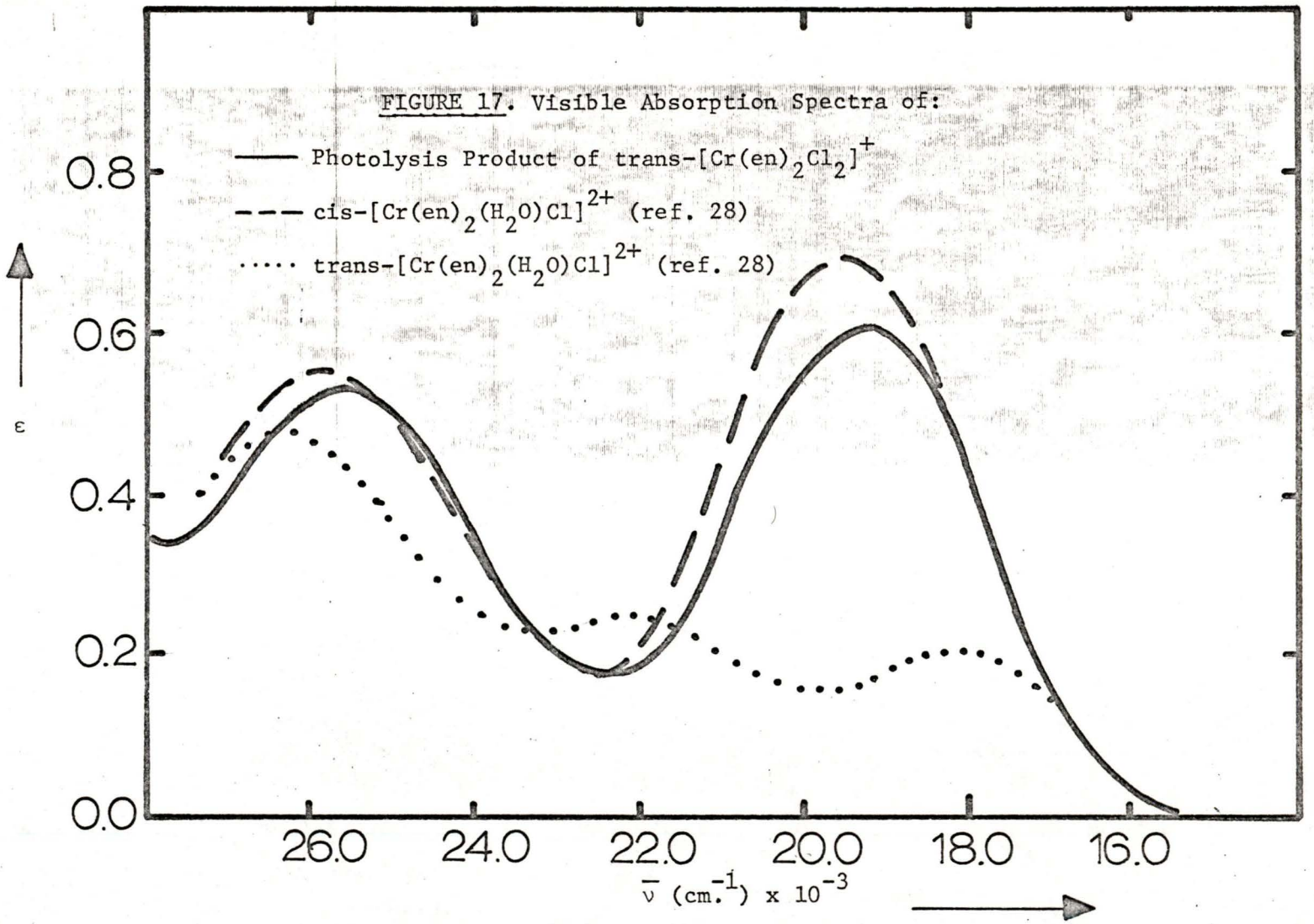
FIGURE 17. Visible Absorption Spectra of:
—— Photolysis Product of trans-[Cr(en)2Cl2]+
– – – cis-[Cr(en)2(H2O)Cl]2+ (ref. 28)
····· trans-[Cr(en)2(H2O)Cl]2+ (ref. 28)
ε
0.8
0.6
0.4
0.2
0.0
26.0
24.0
22.0
20.0
18.0
16.0
ν̄ (cm.-1) x 10-3

D. Photoaquation of trans-$[Cr(en)_2Cl_2]^+$

1. Thermal Reactions

In acidic aqueous solution trans-$[Cr(en)_2Cl_2]^+$ is thermally much more stable than cis-$[Cr(en)_2Cl_2]^+$. The sum of all rate constants for all thermal aquation modes is 9×10^{-5} sec.$^{-1}$ at 35°C as compared to 111×10^{-5} sec.$^{-1}$ for aquation of the cis isomer (27). McDonald and Garner (27) have shown that there are three modes of thermal aquation:

$$\text{trans-}[Cr(en)_2Cl_2]^+ \xrightarrow{k_6} \text{trans-}[Cr(en)_2(H_2O)Cl]^{2+} + Cl^- \qquad (26)$$

$$\xrightarrow{k_7} \text{cis-}[Cr(en)_2(H_2O)Cl]^{2+} + Cl^- \qquad (27)$$

$$\xrightarrow{k_8} \text{trans-}[Cr(en)(H_2O)_2Cl_2]^+ + en \qquad (28)$$

where $k_6 = 6.9 \times 10^{-5}$ sec.$^{-1}$ at 35°C

$k_7 = 1.1 \times 10^{-5}$ sec.$^{-1}$ at 35°C

$k_8 = .8 \times 10^{-5}$ sec.$^{-1}$ at 35°C

It is seen that the predominant reaction is Cl^- aquation with retention of configuration.

2. Identification of Photolysis Products

Separation by ion exchange chromatography (Table 1) of an aqueous solution of trans-$[Cr(en)_2Cl_2]^+$ that had been photolyzed with visible light resulted in the isolation of an orange complex that was identified as cis-$[Cr(en)_2(H_2O)Cl]^{2+}$. Identification was made by comparing the visible absorption spectrum of the complex with that given by McDonald and Garner (28) (Fig. 17).

$$\text{trans-}[Cr(en)_2Cl_2]^+ \xrightarrow{h\nu} \text{cis-}[Cr(en)_2(H_2O)Cl]^{2+} + Cl^- \qquad (29)$$

Other products were found in the separation but in smaller amounts than cis-$[Cr(en)_2(H_2O)Cl]^{2+}$. It is probable that they resulted from secondary photolysis of the primary photolysis product.

It is interesting that photoaquation results predominantly in water substitution cis to the remaining Cl^- while it is the trans position that is labilized. Thermal isomerization from the trans-chloro-aquo to the cis-chloro-aquo isomer following a trans photo-aquation can be ruled out because the rate for this reaction is quite slow ($.6 \times 10^{-5}$ $sec.^{-1}$ at 35^oC (27)) compared to the thermal aquation rate of trans-$[Cr(en)_2Cl_2]^+$ (6.9×10^{-5} $sec.^{-1}$ at 35^oC (27)) which is in turn negligible in comparison to the photolysis rate at 0^oC.

3. Quantum Yields

Photolysis of a 5.0×10^{-3} M aqueous solution of trans-$[Cr(en)_2Cl_2]^+$ at 0^oC and pH 3.0 with visible light resulted in Cl^- aquation with $\phi_a(Cl^-) = (3.1 \pm .2) \times 10^{-1}$ to $(3.5 \pm .2) \times 10^{-1}$ depending on wavelength (Table 2). No ethylenediamine aquation was observed.

TABLE 1

Ion Exchange Chromatography of Cr(III) Complexes

Complex	Charge	Adsorbent	Eluent
$[Cr(en)_2ox]$	1+	Rexyn 102	1×10^{-3} M HCl
$[Cr\ en(H_2O)ox]$	1+	Rexyn 102	1×10^{-3} M HCl
$[Cr\ en(enH)(H_2O)ox]$	2+	Rexyn 102	1×10^{-2} M HCl
$[Cr(enH)(H_2O)(ox)_2]$	0	Dowex-1-X8	1×10^{-3} M $NaClO_4$ [a]
$[Cr\ en(ox)_2]$	1-	Dowex-1-X8	1×10^{-2} M $NaClO_4$
$[Cr(H_2O)(ox)_2]$	1-	Dowex-1-X8	1×10^{-1} M $NaClO_4$
trans-$[Cr(en)_2Cl_2]$	1+	Rexyn-101	3×10^{-1} M HNO_3
cis-$[Cr(en)_2Cl_2]$	1+	Rexyn-101	6×10^{-1} M HNO_3
cis-$[Cr(en)_2(H_2O)Cl]$	2+	Rexyn-101	1 M HNO_3

a. The $NaClO_4$ eluents were all adjusted to pH 3.0

TABLE 2

Aquation Quantum Yields of Cr(III) Complexes in Aqueous Solution at pH 3.0

Complex	Wavelength (n.m.)	Aquation mode	Quantum Yield (mole $E.^{-1}$ x 10) 0°C	15°C	23°C
$[Cr(en)_2ox]^+$	400	en	2.0± .2[a]	1.6± .2	1.7± .2
					1.8± .2
	540	en		1.2± .2	1.4± .2
					1.6± .2
$[Cr\ en(ox)_2]^-$	400	en	.20± .08	.30± .12	
				.20± .09	
	540	en		.20± .08	
cis-$[Cr(en)_2Cl_2]^+$	400	en	1.3± .2		
		Cl^-	.11± .05		
	540	en	1.2± .2	1.2± .2	
		Cl^-	.20± .1		
trans-$[Cr(en)_2Cl_2]^+$	400	Cl^-	3.5± .2		
	424	Cl^-	3.2± .2		
	540	Cl^-	3.2± .2		
	565	Cl^-	3.1± .2[b]		

a. pH 2.0

b. pH 2.5

VIII. DISCUSSION

A. Adamson's Rules

1. Qualitative Predictions

Adamson's Rules correctly predicted the predominant mode of photoaquation for both cis and trans-$[Cr(en)_2Cl_2]^+$ and $[Cr(en)_2ox]^+$ as ethylenediamine, Cl^- and ethylenediamine respectively (Fig. 6). The apparent failure of the rules in predicting oxalate aquation for $[Cr\ en(ox)_2]^-$ while ethylenediamine aquation was observed cannot be unambiguously interpreted for the reasons discussed below.

Porter et al (14) have shown that although $[Cr(ox)_3]^{3-}$ photoracemizes with $\phi_r = 8.0 \times 10^{-2}$ in aqueous solution ϕ_a is less than 1×10^{-3}. This suggests that if the racemization process involves Cr-ox bond breaking followed by immediate rechelation , there is some difficulty in the removal of oxalate from the coordination sphere even if one end of the bidentate oxalate ligand is labilized. If it is assumed that $[Cr\ en(ox)_2]^-$ photoracemizes with about the same $\phi_{racemization}$ as $[Cr(ox)_3]^{3-}$ then ϕ_{total} for $[Cr\ en(ox)_2]^-$ is about 1×10^{-1} (since $\phi_{aquation}$ is about 2×10^{-2}) and the oxalate labilization could account for 80% of this, thus obeying Adamson's Rules.

The above illustrates the importance of considering all modes of photolysis when making comparisons of quantum yields. Lack of knowledge about ϕ_r for $[Cr\ en(ox)_2]^-$ allows only an ambiguous test of Adamson's Rules. It should be noted however that even if ϕ_r is known the ambiguity remains since mechanisms for racemization that do not involve

bond breaking have been postulated.

Another possible explanation for the failure to observe oxalate aquation for $[Cr(en)(ox)_2]^-$ is that a monodentate oxalate ligand may be involved. Chang (29) has reported a stable monodentate protonated oxalate complex of the formula cis-$[Cr(H_2O)_3ox(oxH)]^o$. A solution of this complex gave a negative response to the Fe-salicylate test used to analyse the photolysis solutions for free oxalate. Thus the presence of $[Cr(en)(H_2O)(oxH)ox]^o$ may go undetected in the test for oxalate aquation, but should have been detected in the chromatography.

The formation of this product would be included in ϕ_a measured by pH changes (this work) but would go undetected in ϕ_a measured spectrophotometrically. Oxalate and H_2O are both oxygen coordinating ligands so that the reaction

$$[Cr(en)(ox)_2]^- \xrightarrow{h\nu} [Cr(en)(H_2O)(oxH)ox]^o \qquad (30)$$

would probably produce very little spectral change. Consistent with the above argument ϕ_a measured by pH was higher (2.0×10^{-2}) than that measured spectrophotometrically by Kirk, Moss and Valentin (1.5×10^{-2}) (25). This puts an approximate upper limit of 25% on the maximum percentage of photoaquation giving monodentate oxalate.

It should be understood that the above arguments have been presented in an attempt to rationalize the apparent failure of $[Cr(en)(ox)_2]^-$ to undergo oxalate aquation and merely show that the photoaquation of this

complex cannot be unambiguously interpreted in terms of Adamson's Rules.

2. Quantitative Predictions

Besides predicting the predominant mode of photolysis, Adamson's Rules suggest that the ϕ_a along the labilized axis is about equal to that of a pure O_h complex having the same average field. It is at this point that Adamson's Rules appear to break down.

Cl^- is a weaker field ligand than urea and according to the ΔE rule $[Cr\ Cl_6]^{3-}$ should exhibit a lower ϕ_a than $[Cr\ (urea)_6]^{3+}$ which has $\phi_a = 1.0 \times 10^{-1}$ (22). Adamson's Rules predict that ϕ_a of trans-$[Cr(en)_2Cl_2]^+$ along the Cl^--Cl^- axis should be about the same as ϕ_a for $[Cr\ Cl_6]^{3-}$ and consequently less than 1.0×10^{-1}. In fact ϕ_a for trans-$[Cr(en)_2Cl_2]^+$ is about 3.2×10^{-1}, far higher than predicted.

If Adamson's Rules are interpreted as saying the total ϕ_a is dependent on the average ligand field of all six of the ligands rather than just the average field of the two ligands on the labilized axis, then this part of the Rules merely becomes an extension of the ΔE rule which will be discussed below.

B. The ΔE Rule

The ΔE Rule was successful in predicting the order of the ϕ_a for the series of complex $[Cr(en)_3]^{3+}$, $[Cr(en)_2ox]^+$, $[Cr\ en(ox)_2]^-$ and $[Cr(ox)_3]^{3-}$. ϕ_a decreases with decreasing ligand field strength.

In the case of cis and trans-$[Cr(en)_2Cl_2]^+$ since both complexes have the same average ligand field, one expects similar ϕ_a's. This was not the case. ϕ_a for trans-$[Cr(en)_2Cl_2]^+$ was twice that of cis-$[Cr(en)_2Cl_2]^+$. This disagreement with the ΔE Rule could possibly be corrected by comparing the ϕ_{total} for the two complexes and not just ϕ_a. Until ϕ_i and ϕ_r for cis-$[Cr(en)_2Cl_2]^+$ are known, comparison of the two complexes in terms of the ΔE Rule cannot be justified. Again the importance of considering all modes of photolysis when making comparisons between different complexes is illustrated.

C. Stereochemistry of Photochemical Products

In his review (4) Adamson raises the question as to whether the photoaquation reactions are stereospecific and whether the rules can predict the stereochemistry of the product. He uses the example of $[Cr(NH_3)_5Cl]^{2+}$ and $[Cr(NH_3)_5(SCN)]^{2+}$ in which, if his rules can predict stereochemistry, the trans chloro-aquo and trans thiocyanato-aquo isomers are the predicted photoaquation products. Trans products require that the incoming water approach the complex ion at the position of the labilized leaving group. The cis products would be expected to result from water approaching at a position trans to the labilized position.

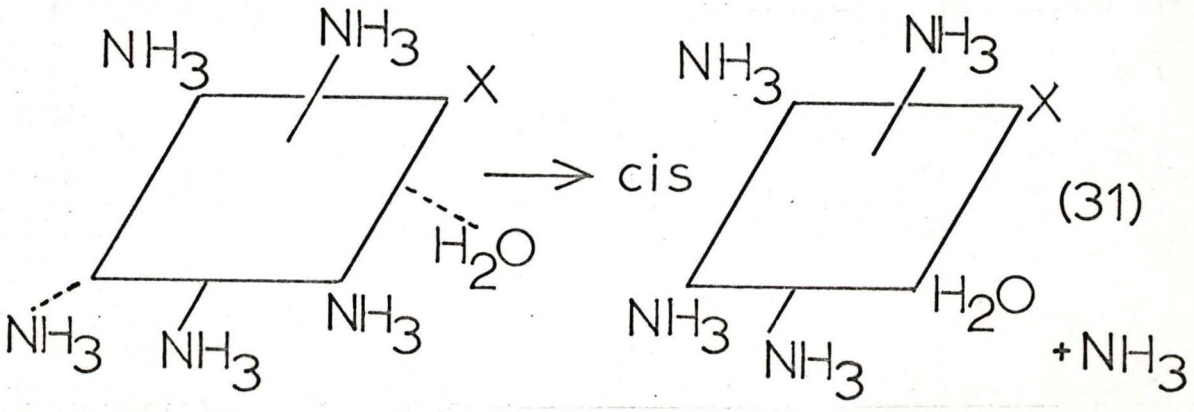

(31)

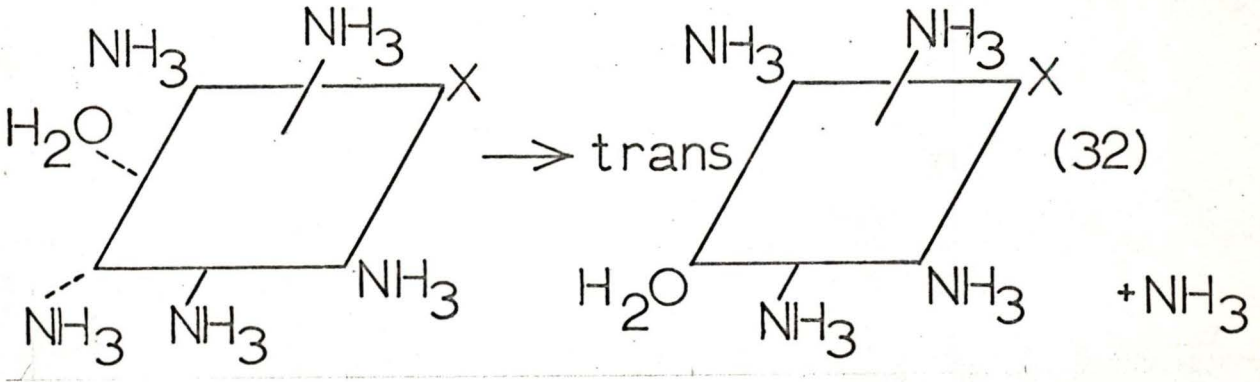

(32)

(where X = Cl^- or SCN^-)

In fact, Schläfer and Wasgestian (30) have reported the cis product for the chloro pentammine and Adamson et al (4) the trans product for the thiocyanato pentammine. It is not clear in the case of the chloro pentammine, however, whether or not the trans product is initially formed and a subsequent post photolysis thermal isomerization occurs giving the cis product.

The present work on trans-$[Cr(en)_2Cl_2]^+$ where the cis chloro-aquo isomer is the photoaquation product suggests that at least in this case the incoming water approaches the ion at positions trans to the leaving group yielding the cis product.

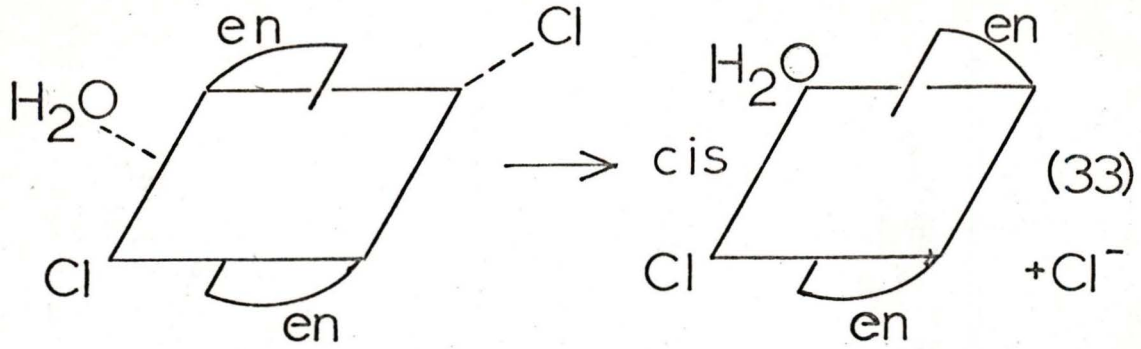

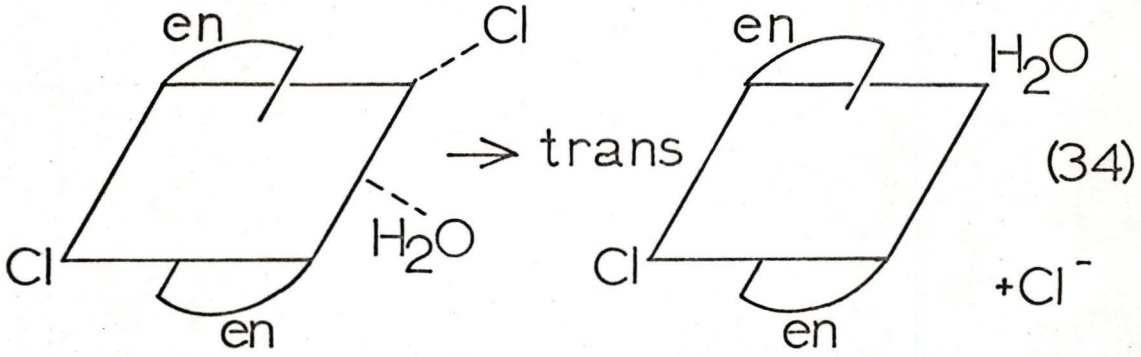

Similarly trans-$[Cr(enH)(H_2O)ox_2]^{o}$ appeared to be the photoaquation product of $[Cr\ en(ox)_2]^{-}$. The only way that this can form is by water attack at a position trans to the labilized leaving group.

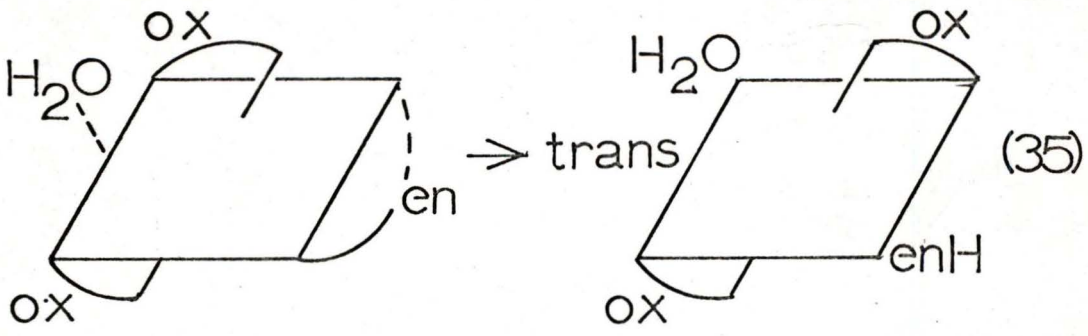

An obvious explanation for the formation of non-stereospecific photoaquation products is that the water attacks the excited complex randomly and not necessarily at the position of the leaving group. Whether the reaction goes by an SN_1 type mechanism involving perhaps a trigonal bipyramidal intermediate or an SN_2 type mechanism is of little consequence since both mechanisms can produce a mixture of stereochemical isomers. It is not absolutely clear at this stage that the photolysis products are not mixtures of isomers, but the formation of non-stereospecific products excludes the possibility of water attacking the excited ion only at the position of the leaving group. Therefore, Adamson's Rules do not in themselves predict the stereochemistry of the photoaquation products.

IX. DISCUSSION OF ERRORS

Due to a number of difficulties the ϕ_a measurements were not sufficiently precise, except in the case of $\phi_a(Cl^-)$ for trans-$[Cr(en)_2Cl_2]^+$, to allow the possibility of small wavelength, temperature or pH dependencies to be investigated.

A. Experimental Difficulties

The rates of the photochemical reactions were dependent on the light intensity which was limited by the low-transmittance of the interference filters. Thus the photochemical reactions proceeded at rates that were in some cases lower than the accompanying thermal reaction at room temperature. Corrections for the thermal reactions introduced large uncertainties into the quantum yield calculations. To eliminate this problem, the photochemical runs were done, where possible, at 0^oC. This however, introduced the problem of measuring pH's and chloride concentrations at 0^oC. The measurements were made using the previously described electrodes but individual measurements were not as precise as those done at room temperature, especially in the case of pH measurements. The combination of the above problems introduced sufficient uncertainty to the quantum yield measurements so that any small variation of ϕ_a with wavelength, temperature or pH would go unnoticed.

B. Non-Linearity of the Rate Plots

The quantum yield calculations were made assuming that the concentration vs. time curves were linear. This is not strictly correct

since the photolysis should ideally follow a first order rate plot in which log (concentration) vs. time is linear. It is, however, convenient to use the concentration vs. time curves rather than the proper first order rate plots.

To a first approximation a plot of concentration vs. time for a first order reaction is linear over the first few percent of reaction. This is displayed in Fig. [18] which was constructed in the following manner. Using an arbitrary first order rate constant ($k = 2.9 \times 10^{-5}$ sec.$^{-1}$ was used in the example since this is of the order of the photolysis rates) the concentration of product at various times was calculated from the first order relationship

$$x = a(1 - e^{-kt})$$

where x = concentration of product

a = initial concentration of reactant

($a = 1.0 \times 10^{-2}$ in the example)

t = time in seconds

The values of x obtained are plotted against time and the points are seen to approximate a straight line very closely over the firt 8% of reaction. Since none of the photolysis reactions went over 5% the approximation used is justified.

C. Calculation of the Uncertainties in ϕ_a

The numerical uncertainties in the rate measurements were found by calculating the probable errors in the least square plots of the photochemical and thermal rate curves from the formula:

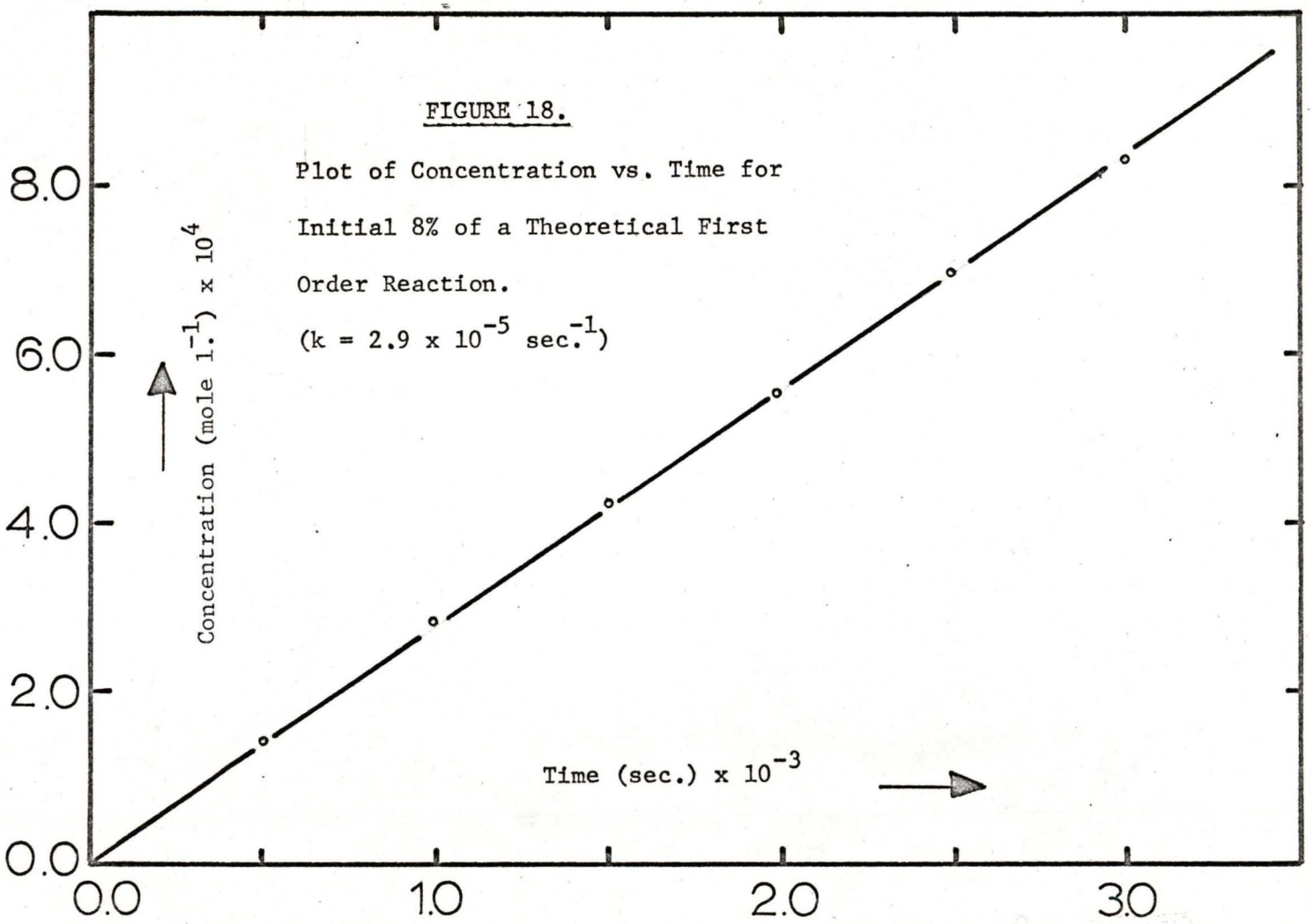

FIGURE 18.

Plot of Concentration vs. Time for Initial 8% of a Theoretical First Order Reaction.

($k = 2.9 \times 10^{-5}$ $sec.^{-1}$)

$$P = 0.6745\sqrt{\frac{\Sigma d^2}{(n-2)\Sigma x^2}}$$

$$\text{where } \Sigma d^2 = \Sigma y^2 - \frac{\Sigma(xy)^2}{\Sigma x^2}$$

Following are examples of quantum yield calculations showing the uncertainties involved (see Fig.11 a, b, c, d):

1. $\phi_a(en)$ of $[Cr(en)_2ox]^+$ at 400 n.m., 23°C, pH 3.0

Overall rate 2.93×10^{-7} mole $l.^{-1}sec.^{-1} \pm .18 \times 10^{-7}$

Thermal rate 1.12×10^{-7} mole $l.^{-1}sec.^{-1} \pm .12 \times 10^{-7}$

Photolysis rate 1.81×10^{-7} mole $l.^{-1}sec.^{-1} \pm \sqrt{(.18)^2+(.12)^2} \times 10^{-7}$

$= 1.81 \times 10^{-7}$ mole $l.^{-1}sec.^{-1} \pm .21 \times 10^{-7}$

% uncertainty in photolysis rate $= \frac{.21}{1.81} \times 10^2 = 11.5\%$

Volume of solution = 5.0 ml.

Photolysis rate (mole $sec.^{-1}$) $= 1.81 \times 10^{-7}$ mole $l.^{-1}sec.^{-1} \times$

5.0×10^{-3} l. (±11.5%)

$= 9.05 \times 10^{-10}$ mole $sec.^{-1}$ (±11.5%)

Average intensity of light absorbed $= 5.12 \times 10^{-9}$ E. $sec.^{-1}$ (±5%)

$$\phi_a(en) = \frac{9.05 \times 10^{-10} \text{ mole sec.}^{-1} (\pm 11.5\%)}{5.12 \times 10^{-9} \text{ E. sec.}^{-1} (\pm 5\%)} = 1.77 \times 10^{-1} \text{ mole E.}^{-1} \left(\pm\sqrt{(11.5\%)^2+(5\%)^2}\right)$$

$$= 1.77 \times 10^{-1} \text{ mole E.}^{-1} (\pm 12.5\%)$$

Thus $\phi_a(en) = (1.8 \pm .2) \times 10^{-1}$ mole $E.^{-1}$

2. ϕ_a(en) of $[Cr\ en(ox)_2]^-$ at 400 n.m., 15°C, pH 3.0

Overall rate $.86 \times 10^{-7}$ mole $l.^{-1}sec.^{-1} \pm .09 \times 10^{-7}$

Thermal rate $.62 \times 10^{-7}$ mole $l.^{-1}sec.^{-1} \pm .05 \times 10^{-7}$

Photolysis rate $.24 \times 10^{-7}$ mole $l.^{-1}sec.^{-1} \pm \sqrt{(.09^2+(.05)^2} \times 10^{-7}$

$= .24 \times 10^{-7}$ mole $l.^{-1}sec.^{-1} \pm .1 \times 10^{-7}$

% uncertainty in photolysis rate $= \frac{.1}{.24} \times 10^2 = 42\%$

Volume of solution used = 5.0 ml.

Photolysis rate (mole $sec.^{-1}$) $= .24 \times 10^{-7}$ mole $l.^{-1}sec.^{-1}$ (±42%) x 5.0×10^{-3} l.

$= 1.20 \times 10^{-10}$ mole $sec.^{-1}$ (±42%)

Average intensity of light absorbed $= 6.53 \times 10^{-9}$ E. $sec.^{-1}$(±5%)

$$\phi_a(en) = \frac{1.20 \times 10^{-10} \text{ mole sec.}^{-1} (\pm 42\%)}{6.53 \times 10^{-9} \text{ E. sec.}^{-1} (\pm 5\%)} = 1.8 \times 10^{-2} \text{ mole E.}^{-1} \left(\pm\sqrt{(42\%)^2 x (5\%)^2}\right)$$

$$= 1.8 \times 10^{-2} \ (\pm 42\%)$$

Thus $\phi_a(en) = (1.8 \pm 0.8) \times 10^{-2}$

3. ϕ_a(en) of cis-$[Cr(en)_2Cl_2]^+$ at 540 n.m., 0°C, pH 3.0

Overall rate 2.99×10^{-7} mole $l.^{-1}sec.^{-1} \pm .40 \times 10^{-7}$

Thermal rate $.04 \times 10^{-7}$ mole $l.^{-1}sec.^{-1} \pm .10 \times 10^{-7}$

Photolysis rate 2.95×10^{-7} mole $l.^{-1}sec.^{-1} \pm \sqrt{(.1)^2+(.4)^2} \times 10^{-7}$

$= 2.95 \times 10^{-7}$ mole $l.^{-1}sec.^{-1} \pm .41 \times 10^{-7}$

% uncertainty in photolysis rate $= \frac{.41}{2.95} \times 10^2 = 14\%$

Volume of solution used = 5.0 ml.

Photolysis rate (mole $sec.^{-1}$) = 2.95×10^{-7} mole $1.^{-1}$ (±14%) x

5.0×10^{-3} 1.

= 1.47×10^{-9} mole $sec.^{-1}$ (±14%)

Average intensity of light absorbed = 1.27×10^{-8} E. $sec.^{-1}$ (±5%)

$$\phi_a(en) = \frac{1.47 \times 10^{-9} \text{ mole sec.}^{-1} (\pm 14\%)}{1.27 \times 10^{-8} \text{ E. sec.}^{-1} (\pm 5\%)} = 1.16 \times 10^{-1} \text{ mole E.}^{-1} \; (\pm\sqrt{(14\%)^2+(5\%)^2})$$

$$= 1.2 \times 10^{-1} \text{ mole E.}^{-1} (\pm 15\%)$$

Thus $\phi_a(en) = (1.2 \pm 0.2) \times 10^{-1}$ mole $E.^{-1}$

4. $\phi_a(Cl^-)$ of trans-$[Cr(en)_2Cl_2]^+$ at 400 n.m., 0°C, pH 3.0

Overall rate 3.07×10^{-7} mole $1.^{-1}sec.^{-1} \pm .05 \times 10^{-7}$

Thermal rate $.005 \times 10^{-7}$ mole $1.^{-1}sec.^{-1} \pm .009 \times 10^{-7}$

Photolysis rate 3.07×10^{-7} mole $1.^{-1}sec.^{-1} \pm\sqrt{(.05)^2+(.009)^2} \times 10^{-7}$

= 3.07×10^{-7} mole $1.^{-1}sec.^{-1} \pm .05 \times 10^{-7}$

% uncertainty in photolysis rate = $\frac{.05}{3.07} \times 10^2 = 1.6\%$

Volume of solution used = 3.29 ml.

Photolysis rate (mole $sec.^{-1}$) = 3.07×10^{-7} mole $1.^{-1}sec.^{-1}$ (±1.6%) x

3.29×10^{-3} 1.

= 9.90×10^{-10} mole $sec.^{-1}$ (±1.6%)

Average intensity of light absorbed = 2.83×10^{-9} E. $sec.^{-1}$ (±5%)

$$\phi_a(en) = \frac{9.90 \times 10^{-10} \text{ mole sec.}^{-1} (\pm 1.6\%)}{2.83 \times 10^{-9} \text{ E. sec.}^{-1} (\pm 5\%)} = 3.5 \times 10^{-1} \text{ mole E.}^{-1} \; (\pm\sqrt{(1.6\%)^2+(5\%)^2})$$

$$= 3.5 \times 10^{-1} \text{ mole E.}^{-1} (\pm 5.3\%)$$

Thus $\phi_a(en) = (3.5 \pm .2) \times 10^{-1}$ mole $E.^{-1}$

D. The Inner Filter Effect

Corrections for inner filter effects must be applied when significant amounts of product are formed in the photolysis.

Consider the reaction:

$$[A] \xrightarrow{h\nu} [B] \qquad (35)$$

As the concentration of B increases the complex B absorbs more and more of the incident light. This has the effect of reducing the intensity of light available to A. Sophisticated treatments for inner filter corrections have been developed (31). The following simplified treatment will show that the inner filter correction necessary for results in this work is small, except in the case of trans-$[Cr(en)_2Cl_2]^+$.

The 5.3% uncertainty in $\phi_a(Cl^-)$ for trans-$[Cr(en)_2Cl_2]^+$ is low enough so that inner filter effects are not negligible compared to the uncertainty. Following is the correction applied for inner filter effects.

Initial concentration of trans-$[Cr(en)_2Cl_2]^+$ = 1.00×10^{-2}

Total change in $[Cl^-]$ during photolysis = 2.08×10^{-4}

Concentration of product at the end of photolysis =

Total change in $[Cl^-]$ during photolysis = 2.08×10^{-4}

Molar extinction coefficient of cis-$[Cr(en)_2(H_2O)Cl]^{2+}$

at 400 n.m. = 50 (Fig. 17)

Absorbance of 2.08×10^{-4} M cis-$[Cr(en)_2(H_2O)Cl]^{2+}$

$= 2.08 \times 10^{-4} \times 50 = 1.04 \times 10^{-2}$

% Absorbance = 100 - % Transmittance = 2.3%

Thus the maximum percent of light absorbed by the cis-$[Cr(en)_2(H_2O)Cl]^{2+}$ is 2.3%. This figure can be used as the upper limit of the inner filter correction necessary. In most cases the inner filter corrections will be much smaller than this. This particular case gives an unusually high inner filter correction because the molar extinction coefficient of the product at the wavelength of photolysis is higher than that of the reactant. In all other cases this relationship is reversed.

Application of the inner filter correction changes the $\phi_a(Cl^-)$ by only a small amount.

$\phi_a(Cl^-)$ (without correction) $= (3.5 \pm .2) \times 10^{-1}$

$\phi_a(Cl^-)$ (with correction) $= (3.5 \pm .2) \times 10^{-1} \times 1.023$

$= (3.6 \pm .2) \times 10^{-1}$

X. SUMMARY AND CONCLUSION

It has been shown that the products of photoaquation of the complex ions $[Cr(en)_2ox]^+$ and $[Cr\ en(ox)_2]^-$ are protonated monodentate ethylenediamine complexes.

$$[Cr(en)_2ox]^+ \xrightarrow{h\nu} [Cr(enH)en(H_2O)ox]^{2+} \qquad (36)$$

$$[Cr\ en(ox)_2]^- \xrightarrow{h\nu} trans\text{-}[Cr(enH)(H_2O)ox_2]^o \qquad (37)$$

The series of complexes $[Cr(en)_3]^{3+}$, $[Cr(en)_2ox]^+$, $[Cr\ en(ox)_2]^-$ and $[Cr(ox)_3]^{3-}$ were shown to obey the ΔE Rule in that the aquation quantum yields increase with increasing ΔE. Adamson's Rules correctly predicted ethylenediamine aquation for $[Cr(en)_2ox]^+$, but could not be unambiguously interpreted for $[Cr\ en(ox)_2]^-$, where oxalate aquation was predicted, but ethylenediamine aquation observed.

Adamson's Rules were correct in predicting ethylenediamine aquation for cis-$[Cr(en)_2Cl_2]^+$ and Cl^- aquation for trans-$[Cr(en)_2Cl_2]^+$. The quantitative predictions of Adamson's Rules failed in suggesting that trans-$[Cr(en)_2Cl_2]^+$ should have a low $\phi_a(Cl^-)$ when a relatively high $\phi_a(Cl^-)$ was found.

The stereochemistry of the photoaquation products of trans-$[Cr(en)_2Cl_2]^+$ and $[Cr\ en(ox)_2]^-$ showed that non-stereospecific substitution occurs at least in these two cases.

XI. SUGGESTIONS FOR FURTHER WORK

1. An interesting series of Cr(III) complexes with varying Δ's has recently been reported (32). In order of decreasing Δ the series is: $[Cr(NH_3)_5Cl]^{2+}$, $[Cr(methylamine)_5Cl]^{2+}$, $[Cr(propylamine)_5Cl]^{2+}$, $[Cr(ethylamine)_5Cl]^{2+}$, $[Cr(butylamine)_5Cl]^{2+}$. It would be of interest to measure the aquation quantum yields of this series to see if the ΔE Rule is obeyed. One attractive feature of this series is that all of the ligands are monodentate making interpretation of the photolysis reactions less difficult than when bidentate ligands are involved. The complexes are sufficiently stable in aqueous solution for study. The only disadvantage immediately apparent is the low solubility of the higher molecular weight complexes in water.

2. The photolysis products of both cis and trans-$[Cr(en)_2Cl_2]^+$ should be studied more closely by ion exchange chromatography to establish the following:

a) whether the reaction

$$cis\text{-}[Cr(en)_2Cl_2]^+ \xrightarrow{h\nu} trans\text{-}[Cr(en)_2Cl_2]^+ \qquad (38)$$

occurs with appreciable efficiency.

b) the stereochemistry of the photoaquation products of cis-$[Cr(en)_2Cl_2]^+$.

c) whether the reaction

$$trans\text{-}[Cr(en)_2Cl_2]^+ \xrightarrow{h\nu} trans\text{-}[Cr(en)_2Cl(H_2O)]^+ \qquad (39)$$

occurs with appreciable efficiency. At present it has only been established that $cis\text{-}[Cr(en)_2(H_2O)Cl]^{2+}$ is the major product of photolysis.

XII. BIBLIOGRAPHY

1. "Advances in Chemistry Series", Ed. R.F. Gould, American Chemical Society Publications, (1967), vol. 62, p. 32.

2. F. Basolo, R.G. Pearson, "Mechanisms of Inorganic Reactions", second edition, John Wiley and Sons, (1967), p. 129.

3. F. Basolo, R.G. Pearson, ibid, p.290

4. A.W. Adamson, et al, Chem. Reviews, 68, 541, (1968).

5. D. Valentine Jr., "Advances in Photochemistry", Ed. W.A. Noyes, et al, Interscience Publishers, (1968), vol. 6, p. 123

6. L.E. Orgel, "Introduction to Transition Metal Chemistry", second edition, Methuen and Co., (1966), p. 98.

7. L.S. Forster, "Transition Metal Chemistry", Ed. Carlin, Interscience Publishers, (1969), vol. 5, p. 1.

8. M.R. Edelson, R.A. Plane, J. Phys. Chem., 63, 327, (1959).

9. H.L. Schläfer, J. Phys. Chem., 69, 2201, (1965).

10. A.W. Adamson, J. Phys. Chem., 71, 798, (1967).

11. G.B. Porter, Private communication.

12. M.R. Edelson, R.A. Plane, Inorg.Chem., 3, 231, (1964).

13. H.L. Schlafer, W. Geis, Z.Phys. Chem. (Frankfurt), 65, 107, (1969).

14. G.B. Porter, et al, J. Am. Chem. Soc., 84, 4027, (1962).

15 C.J. Ballhausen, "Introduction to Ligand Field Theory", McGraw-Hill, (1962), p. 24.

16. F.A. Cotton, G.Wilkinson, "Advanced Inorganic Chemistry", Interscience Publishers, (1967).

17. H.L. Schläfer, et al, Z. Phys. Chem., 24, 307, (1960).

18. E. Bushra, C.H. Johnson, J. Chem. Soc., 1939, 1937, (1939).

19. G. Brauer, "Handbook of Preparative Inorganic Chemistry", second edition, Academic Press, (1965), vol. 2, p. 1357.

20. "Inorganic Synthesis", Ed. W.C. Fernelius, McGraw-Hill Inc., (1946), vol. 2, p. 201.

21. J Lee, H.H. Seliger, J. Chem. Phys., 40, 519, (1964).

22. A.W. Adamson, E.E. Wegner, J. Am. Chem. Soc., 88, 394, (1966).

23. F. Buriel-Marti, et al, Analytical Chemistry, 25, 583, (1953).

24. D.A. House, et al, Inorg. Chem., 7, 749, (1968).

25. A.D. Kirk, K.C. Moss, J.G. Valentin, in press.

26. R.E. Hamm, et al, J. Am. Chem. Soc., 83, 340, (1961).

27. D.J. McDonald, C.S. Garner, Inorg. Chem., 1, 20, (1962).

28. D.J. McDonald, C.S. Garner, J. Am. Chem. Soc., 83, 4152, (1961).

29. J.C. Chang, Inorg. Nucl. Chem. Letters, 5, 587, (1969).

30. H.L. Schläfer, H.F. Wasgestian, Z. Phys. Chem., 57, 3, (1968).

31. H.L. Schläfer, et al, Berichte der Bunsengesellschaft, 67, 883, (1963).

32. M. Parris, W.J. Wallace, Can. J. Chem., 47, 2257, (1969).

XIII. APPENDIX

The Franck-Condon Principle

Referring to fig. 5, the Franck-Condon principle is equivalent to the requirement that all electronic transitions occur vertical to the internuclear separation axis. Electronic transitions take place much more rapidly than molecular vibrations. Thus the spacial coordinates of the complex ion remain unchanged during electronic transitions and unless the potential energy curves of the upper and lower states have the same shape and position along the internuclear separation axis, electronic excitations, which normally originate from the zeroth vibrational level of the lower state, will go to high vibrational levels of the upper state. Similar arguments can be made for de-excitation processe such as phosphorescence, fluorescence, and non-radiative transitions.

Surname: VALENTIN Given Names: JOHN GWYNFRYN

Place of Birth: ENGLAND Date of Birth: May 2, 1942

Educational Institutions Attended, with Dates of Entering and Leaving:

UNIVERSITY OF BRITISH COLUMBIA, VANCOUVER	1960	to	1964
UNIVERSITY OF VICTORIA, VICTORIA	1968	to	1970
		to	

Degrees, Diplomas, Etc. Awarded, with Dates and Names of Institutions:

B.Sc. (Honors)	1964	University of British Columbia, Vancouver

Honors and Awards:

N.R.C. Grants, 1968/69 and 1969/70

Government of B.C. - First Class Scholarship 1963/64

Government of B.C. - Second Class Scholarships 1962/63 and 1961/62

Imperial Order of Oddfellows Bursary 1960/61

Publications:

1. J. G. Hooley, W. P. Garby, J. G. Valentin,
"The Effect of Sample Size and Shape on the Bromination of Graphite",
Carbon 3, 7 - 16, (1965)

2. A. D. Kirk, K. C. Moss, J. G. Valentin,
"The Separation, Identification and Estimation of Cr(III) Complex Ions by Thin Layer Chromatography and Diffuse Reflectance Spectroscopy", J. Chromatog., 36, 332 - 337, (1968).

THE UNIVERSITY OF VICTORIA LIBRARY

MANUSCRIPT THESIS

AUTHORITY TO DISTRIBUTE

AUTHOR: This thesis may be lent or microfilm copies made available:

(signature of the author in one of the spaces below)

(a) Without restriction ---[redacted]

(b) With the restriction that, for a period of five years (until _____) the
Date
written approval of the following is required:

(1) The Chairman, School of Graduate Studies _____

(2) The Author _____

(3) both the Chairman, School of Graduate Studies, and the Author _____

BORROWERS: The borrower undertakes, by signing below, to give proper credit for any use made of the thesis, and to obtain the consent of the author if it is proposed to make extensive quotations, or to reproduce the thesis in whole or in part.

Signature of Borrower	Address	Date